J. Fluid Mech. (1982), *vol.* 116, *pp.* 315–342
Printed in Great Britain

The stability of quasi-geostrophic fields induced by potential vorticity sources

By LEE-OR MERKINE
Department of Mathematics, Technion-Israel Institute of Technology, Haifa

(Received 17 March 1980 and in revised form 8 June 1981)

The stability of quasi-geostrophic barotropic fields induced by localized finite-amplitude potential vorticity sources or topographies which depend only on the zonal direction is investigated both analytically and numerically. The analytical study is for weak forcing. It demonstrates that the field induced by the topography is stable whereas the field induced by the potential vorticity source can be unstable. The growth rate is exponential and is a function of both nonlinearity and friction. In the absence of friction the flow field is always unstable. The instability takes the form of a current whose meridional wavenumber is that of a stationary Rossby wave. In the zonal direction the current exhibits long-scale oscillations and exponential decay. The numerical computations which are for strong forcing verify all the indications of the asymptotic study. They show a rapid exponential growth of a non-propagating but oscillatory wave packet whose location is fixed relative to the forcing. The zonal scale of the packet is that of a stationary Rossby wave. For weak forcing the instability can be responsible for changing the flow field from one quasi-steady state to another where the energy extraction takes place in the region of the source. It is efficient for potential vorticity sources whose length scale is comparable to the length scale of stationary Rossby waves. In agreement with the asymptotic study, fields induced by strong topographic forcing are found to be stable. The asymptotic analysis is also applied to baroclinic flows where the investigation is performed in the framework of the two-layer model. It is demonstrated that the same mechanism which operates in barotropic systems can also destabilize baroclinic flows which possess subcritical shears.

1. Introduction

The influence of topography and heat sources on the evolution of quasi-geostrophic systems is a central problem of geophysical fluid dynamics. A few years ago there was a flare-up of papers that were concerned with the nature of large-scale flow past topographic features with some emphasis on the Taylor-column problem. We do not attempt to provide the reader with an exhaustive list of references but some examples are Hogg (1973); Huppert (1975); McCartney (1975) and Merkine (1975).

In most cases the studies were concerned with steady-state solutions. The problem of the stability of such solutions to small perturbations has not been dealt with. The difficulty is obvious; because of the non-separability of the equation it is not easy to study the stability of general fields which are strongly nonhomogeneous in the direction of the basic velocity. The exceptional situation occurs when the nonhomogeneity is wave-like in nature. Then, Fourier-series representation of the perturbation field or

the use of Floquet's theorem leads to a tractable analytical investigation. Indeed, this is the approach adopted by Lorenz (1972); Gill (1974*a*); Coaker (1977) and others in their investigation of the stability of Rossby waves.

The need for stability studies of more general nonhomogeneous fields in quasi-geostrophic systems became more acute when Charney & Devore (1979) suggested the existence of multiple flow equilibria in the atmosphere. Using the quasi-geostrophic barotropic vorticity equation in a highly truncated spectral form and introducing zonally asymmetric fields induced by topography and by a barotropic analogue of thermal driving they found the existence of several equilibrium states. In some instances two stable and one unstable equilibrium states were found. The transition among the equilibrium states occurred via an instability mechanism owing its existence to the asymmetric forcing. The close resemblance of the equilibrium states found by Charney & Devore to familiar flow configurations of the atmosphere tends to support their conclusions in spite of the severe spectral truncation of their model.

Motivated by the above studies we seek to determine the conditions leading to instabilities that grow in place in quasi-geostrophic fields induced by localized potential vorticity sources. The sources can be attributed to large-scale physical processes not resolved by the simplified model considered. As a first step towards studying more general fields we consider basic states which are nonhomogeneous in the streamwise direction only. This simplification allows us to obtain with relative ease exact finite-amplitude steady-state solutions of the governing nonlinear equations.

The stability study is guided by the important work of Mahony (1972) who investigated the instability mechanism leading to the generation of cross waves in a long water channel excited at one end by a wave maker. Analytical approach to the stability problem is possible when nonlinearity, which measures the nonhomogeneity of the basic field and which is also proportional to the strength of the potential vorticity source, is weak. As a result small growth rates are obtained. Nevertheless, the good agreement of Mahony's asymptotic study with the experimental results of Barnard & Pritchard (1972) do support the relevance of such an approach. In §2 the asymptotic investigation is performed and instability is found. It is discussed in §3; and §4 presents numerical computations of the instability when the nonhomogeneity of the basic field is strong. The results show a rapid evolution of a non-propagating wave packet.

The analysis described in §§2–4 is restricted to barotropic flows. Section 5 extends the asymptotic analysis of §2 to two-layer baroclinic flows possessing subcritical shears.

2. Analysis

Consider a quasi-geostrophic barotropic flow in a horizontally open domain which is confined vertically by two horizontal planes, a distance D apart. The beta plane approximation is employed; f_0 is the Coriolis parameter at the reference latitude and β' is the gradient of the planetary vorticity at that latitude. The flow field consists of a uniform westerly flow U^* plus a deviation induced by a localized potential vorticity source and by a localized topography. The nondimensional quasi-geostrophic vorticity equation govening the deviation stream function ψ is

$$\nabla^2\psi_t + \nabla^2\psi_x + \beta\psi_x + F_x + r\nabla^2\psi + \epsilon J(\psi, \nabla^2\psi + F) = G. \tag{1}$$

U^* and L are the scales chosen for nondimensionalization where the actual value of L will be specified later; x points eastward and y points northward; $\beta = \beta' L^2/U^*$ is the beta parameter, $r = E^{\frac{1}{2}}/Ro$ is the friction parameter where $Ro = U^*/(f_0 L)$ is the Rossby number and $E = \nu/(f_0 D^2)$ is the Ekman number; ϵ measures the importance of nonlinear effects. It is equal to $\max(\alpha/Ro, (f_0 \tau Ro)^{-1})$, where α is the fractional height of the topography and τ is the time scale of the vorticity source. F and G denote the shape functions of the topography and of the potential vorticity source, respectively, where $\max|F| \leqslant 1$ and $\max|G| \leqslant 1$. The dimensional deviation stream function is given by $\epsilon U^* L\psi$. Large-scale geophysical flows are typified by small Rossby numbers and consistent quasi-geostrophic approximation requires that β, r and ϵ remain bounded in the limit $Ro \to 0$. We shall consider the case of $r \ll 1$ since the spin-down time for geophysical flows is much larger than the advection time.

Assume that $F = F(x)$ and $G = G(x)$ and let $\phi(x)$ be the corresponding steady-state solution. It follows that $J(\phi, \nabla^2\phi + F) \equiv 0$ and that ϕ is governed by the linear equation

$$\phi_{xxx} + \beta\phi_x + F_x + r\phi_{xx} = G(x), \tag{2}$$

for *finite* values of ϵ. ϕ is the basic state whose stability properties we wish to determine. Using the Fourier transform

$$\hat{f}(k) = \frac{1}{(2\pi)^{\frac{1}{2}}} \int_{-\infty}^{\infty} dx\, e^{-ikx} f(x), \tag{3}$$

we find that

$$\hat{\phi}(k) = \frac{\hat{F}(k)}{(k^2 - \beta - ikr)} + \frac{i\hat{G}(k)}{k(k^2 - \beta - ikr)}. \tag{4}$$

It will be demonstrated later that the relevant information concerning the stability properties of ϕ can be extracted directly from (4) and there is no need to embark on the difficult although possible task of transforming $\hat{\phi}$ back into the physical plane. It can be shown, however, that the basic state consists of a local response confined to the vicinity of the forcing plus a Rossby lee wave. Unlike the stability studies of Gill (1974*a*) and Coaker (1977) an instability which grows in place is intrinsic to the local field and not to the Rossby wave.

Let

$$\psi = \phi(x) + \varphi(x, y, t), \tag{5}$$

where φ is the perturbation from the steady-state solution ϕ. Upon substituting (5) into (1) and neglecting quadratic terms of the perturbation field we obtain the following linear equation for φ,

$$\nabla^2\varphi_t + \nabla^2\varphi_x + \beta\varphi_x + r\nabla^2\varphi + \epsilon\phi_x\nabla^2\varphi_y - \epsilon(\phi_{xxx} + F_x)\,\varphi_y = 0. \tag{6}$$

Without any loss of generality we can write

$$\varphi(x, y, t) = U(x, t)\sin ly + V(x, t)\cos ly, \tag{7}$$

where l, the meridional wavenumber, is still unspecified. When (7) is substituted into (6) we obtain two equations governing the evolution of U and V,

$$U_{xxt} - l^2U_t + U_{xxx} - l^2U_x + \beta U_x + r(U_{xx} - l^2U) = \epsilon l\phi_x(V_{xx} - l^2V) - \epsilon l(\phi_{xxx} + F_x)\,V, \tag{8}$$

$$V_{xxt} - l^2V_t + V_{xxx} - l^2V_x + \beta V_x + r(V_{xx} - l^2V) = -\epsilon l\phi_x(U_{xx} - l^2U) + \epsilon l(\phi_{xxx} + F_x)\,U. \tag{9}$$

The difficulty in solving the last two equations lies in the fact that the terms proportional to ϵ contain coefficients which are functions of x of which ϕ is not even explicitly known. This problem can be alleviated if instead of dealing directly with (8) and (9) we study the time evolution of their Fourier transforms given by

$$\hat{U}_t + i\Omega(k)\,\hat{U} + r\hat{U} = -\frac{\epsilon l i}{(k^2+l^2)}\frac{1}{(2\pi)^{\frac{1}{2}}}\int_{-\infty}^{\infty} dk'(k-k') \times \{(k^2-2kk'-l^2)\,\hat{\phi}(k-k') - \hat{F}(k-k')\}\hat{V}(k',t), \quad (10)$$

$$\hat{V}_t + i\Omega(k)\,\hat{V} + r\hat{V} = \frac{\epsilon l i}{(k^2+l^2)}\frac{1}{(2\pi)^{\frac{1}{2}}}\int_{-\infty}^{\infty} dk'(k-k') \times \{(k^2-2kk'-l^2)\,\hat{\phi}(k-k') - \hat{F}(k-k')\}\hat{U}(k',t), \quad (11)$$

where

$$\Omega(k) = k(1-\beta/(k^2+l^2)) \quad (12)$$

is the Rossby wave dispersion relation.

Analytical study of the stability problem is feasible only for small values of ϵ. Then, the nonhomogeneity of the basic field seems to affect the evolution of the disturbance at large time only and we can exploit this separation of scales to our advantage. Thus, we formally expand $\hat{U}$ and $\hat{V}$ in powers of ϵ in the following way:

$$\hat{U} = U^0 + \epsilon U' + \ldots, \quad \hat{V} = V^0 + \epsilon V' + \ldots. \quad (13)$$

It will be seen that this expansion collapses for $t = O(\epsilon^{-\frac{3}{2}})$ and that a modified expansion is required. Nevertheless, we choose to start with (13) since its breakdown provides us with the physical understanding required for devising a more uniform asymptotic expansion. It should be emphasized again that the basic field is an exact solution of the governing equation independently of ϵ and it requires no approximation. The difficulty is associated with the stability study.

The solution for the leading order of the perturbation field is

$$U^0(k,t) = \gamma(k)\,e^{-i\Omega(k)t}e^{-rt}, \quad V^0(k,t) = \delta(k)\,e^{-i\Omega(k)t}e^{-rt}, \quad (14)$$

which describes the spectrum of free Rossby waves whose decay rate r is independent of the wavenumber vector. γ and δ determine the initial spectrum distribution. Thus, to this order in ϵ the nonhomogeneity of the basic field is not felt, implying that only higher-order terms in ϵ could reveal a growing perturbation. In the modified expansion the nonhomogeneity of the basic field is incorporated directly into the leading order of the expansion. This enables the free Rossby waves and the growing perturbation to bootstrap one another to yield an exponentially growing wave packet.

The next order of the expansion is governed by

$$U'_t + i\Omega(k)\,U' + rU' = -\frac{li}{(k^2+l^2)}\frac{e^{-rt}}{(2\pi)^{\frac{1}{2}}}\int_{-\infty}^{\infty} dk' \times [(k-k')\,Y(k,k') + Z(k,k')]\,\delta(k')\,e^{-i\Omega(k')t}, \quad (15)$$

$$V'_t + i\Omega(k)\,V' + rV' = \frac{li}{(k^2+l^2)}\frac{e^{-rt}}{(2\pi)^{\frac{1}{2}}}\int_{-\infty}^{\infty} dk' \times [(k-k')\,Y(k,k') + Z(k,k')]\,\gamma(k')\,e^{-i\Omega(k')t}, \quad (16)$$

where the right-hand side of (15) and (16) is obtained by substituting (14) into the right-hand side of (10) and (11):

$$Y(k,k') \equiv \left[\frac{(k^2-2kk'-l^2)}{(k-k')^2-\beta-i(k-k')r}-1\right]\hat{F}(k-k'),$$

$$Z(k,k') \equiv \frac{i(k^2-2kk'-l^2)\,\hat{G}(k-k')}{(k-k')^2-\beta-i(k-k')r}. \tag{17}$$

Y is the contribution due to the topography and Z is the contribution arising from the potential vorticity source. The solution for U' and V' is simply

$$U' = -\frac{li}{(k^2+l^2)}e^{-i\Omega(k)t}e^{-rt}\frac{1}{(2\pi)^{\frac{1}{2}}}\int_0^t ds\, e^{i\Omega(k)s}\int_{-\infty}^{\infty}dk' \times[(k-k')\,Y(k,k')+Z(k,k')]\,\delta(k')\,e^{-i\Omega(k')s}, \tag{18}$$

$$V' = \frac{li}{(k^2+l^2)}e^{-i\Omega(k)t}e^{-rt}\frac{1}{(2\pi)^{\frac{1}{2}}}\int_0^t ds\, e^{i\Omega(k)s}\int_{-\infty}^{\infty}dk' \times[(k-k')\,Y(k,k')+Z(k,k')]\,\gamma(k')\,e^{-i\Omega(k')s}. \tag{19}$$

It is clear that the formal expansion in ϵ gives a useful description of the solution provided the $O(\epsilon)$ correction remains bounded in time. This may not be the case, as the following considerations demonstrate. For any finite value of t the expressions given by (18) and (19) are bounded, yielding an $O(\epsilon)$ correction to the leading order given by (14). Thus, it suffices to consider the behaviour of (18) and (19) for large time which amounts to considering the integrand of the outer integral for large values of s. This integrand contains the inner integral as a part of it. For large s the inner integral can be estimated using the method of stationary phase.

Stationary phase is obtained by requiring that

$$\frac{d\Omega}{dk'} = 1-\beta\frac{l^2-k'^2}{(k'^2+l^2)^2} = 0, \tag{20}$$

where Ω is given by (12). This requirement is equivalent to seeking waves with zero group velocity. Real solutions of (20) are possible provided $l^2 \leqslant \beta$. They are given by

$$k_0' = \pm 2^{-\frac{1}{2}}[-(2l^2+\beta)+\beta^{\frac{1}{2}}(\beta+8l^2)^{\frac{1}{2}}]^{\frac{1}{2}}. \tag{21}$$

The second derivative of Ω with respect to k' is given by

$$\frac{d^2\Omega}{dk'^2} = \beta\frac{2k'(3l^2-k'^2)}{(k'^2+l^2)^3}. \tag{22}$$

In general (22) is different from zero for $k' = k_0'$ given by (21) unless $l^2 = \beta$. In this latter case both (20) and (22) vanish with $k_0' = 0$, $\Omega(0) = 0$ and

$$\frac{d^3}{dk'^3}\,\Omega(k_0' = 0, l^2 = \beta) = \frac{6}{\beta}.$$

The dominant contribution to the inner integral comes from the phase which is most stationary. This requires $l^2 = \beta$ thus determining the most dangerous meridional wavenumber. Dimensionally it is given by $l^* = (\beta'/U^*)^{\frac{1}{2}}$ which is also the wavenumber of a stationary Rossby wave. These considerations imply that $(U^*/\beta')^{\frac{1}{2}}$ is the natural

length scale of the problem and we identify it with L. With this renormalization we obtain that $\beta = 1$ and l is set equal to 1.

The method of stationary phase yields the following estimates for the inner integrals appearing in (18) and (19)

$$\int_{-\infty}^{\infty} dk'[(k-k')\,Y(k,k')+Z(k,k')]\begin{pmatrix}\delta(k')\\ \gamma(k')\end{pmatrix} e^{-i\Omega(k')s}$$

$$\sim [kY(k,0)+Z(k,0)]\begin{pmatrix}\delta(0)\\ \gamma(0)\end{pmatrix} I, \quad s\to\infty, \quad (23)$$

with

$$I = \int_{-\infty}^{\infty} dk' \exp(-ik'^3 s) = 3^{-\frac{1}{2}}\Gamma(\tfrac{1}{3})\, s^{-\frac{1}{3}} \quad (24)$$

from Gradshteyn & Ryzhik (1965).

It follows that the $O(\epsilon)$ correction is given by

$$\begin{pmatrix}U'\\ V'\end{pmatrix} \sim e^{-i\Omega(k)t}e^{-rt}\begin{pmatrix}-\delta(0)\\ \gamma(0)\end{pmatrix}\frac{\Gamma(\frac{1}{3})}{(6\pi)^{\frac{1}{2}}}\frac{i}{(k^2+1)}$$

$$\times [kY(k,0)+Z(k,0)]\int_0^t ds\, e^{i\Omega(k)s}s^{-\frac{1}{3}}, \quad t\to\infty. \quad (25)$$

The only way that the perturbation expansion breaks down is when the last integral becomes large. This is possible only if $\Omega(k) = 0$, i.e. for long waves ($k \sim 0$) or equivalently for that part of the spectrum which represents currents. We obtain that for the long-wave part of the spectrum the $O(\epsilon)$ correction to the perturbation field is given by

$$\begin{pmatrix}U'\\ V'\end{pmatrix} \sim e^{-rt}\begin{pmatrix}\delta(0)\\ -\gamma(0)\end{pmatrix}\frac{\Gamma(\frac{1}{3})}{(6\pi)^{\frac{1}{2}}}\hat{G}(0)\,(\tfrac{3}{2}t^{\frac{2}{3}}). \quad (26)$$

For any other value of k the integrand is oscillatory and the Riemann–Lebesgue lemma guarantees that the integral is not large. The above solution for the perturbation field can be interpreted as representing a group-velocity resonance where two perturbation fields with zero group velocity interact with the long-wave part of the spectrum of the forced (basic) flow. This triad of wave vectors is shown in figure 1.

We would like to point out that the estimate given by (26) could have been achieved differently. Starting again with (18) and (19), we can perform the s integration first and then use the method of stationary phase to estimate the integral over k' for large t. The end result is the same. We also note that the contribution of the stationary points (21) for which $l^2 < \beta$ and hence (22) does not vanish leads to a correction which is $O(\epsilon t^{\frac{1}{2}})$ and consequently insignificant compared to (26).

It is important to mention that the estimate of the integral as presented above is not complete since it omits a possible resonant instability of the wavy part of the wake of the basic flow.† The Rossby lee wave is associated with the roots of the denominator of (4). When $r \ll 1$ these roots are located close to the real axis in the complex k plane. This suggests that for times much less than the spin-down time ($t \ll r^{-1}$) the perturbation field can interact efficiently with the Rossby lee wave. The two perturbation components centred within a distance of $O(r)$ around the wave vectors $\bar{K}_1 = (\frac{1}{2}, 3^{\frac{1}{2}}/2)$, $\bar{K}_2 = (\frac{1}{2}, -3^{\frac{1}{2}}/2)$ and frequencies $\Omega(\bar{K}_1) = 0$, $\Omega(\bar{K}_2) = 0$

† The author is indebted to Dr Peter Rhines for this comment.

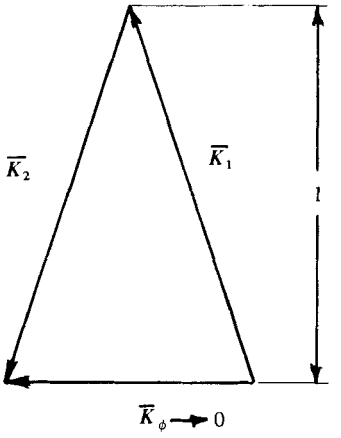

FIGURE 1. Triad of waves participating in the zero group-velocity resonance. $\mathbf{K}_1$ and $\mathbf{K}_2$ are the wave vectors of the perturbation field and $\mathbf{K}_\phi$ which tends to zero is the wave vector of the basic flow.

form with the Rossby lee wave, whose wave vector and frequency are $\bar{K}_\phi = (1, 0)$, $\Omega(\bar{K}_\phi) = 0$, a resonant triad for which the $O(\epsilon)$ spectrum of the perturbation field is proportional to t/r. ($\bar{K} \equiv (k, l)$ and $\beta = 1$.) Under a more uniform perturbation sequence this linear growth can become exponential, suggesting instability of the Rossby lee wave. Since $\partial\Omega(\bar{K}_1)/\partial k = \frac{1}{2}$, $\partial\Omega(\bar{K}_2)/\partial k = \frac{1}{2}$ this possible instability is convective, contrary to the non-convective nature (zero group-velocity) of the instability investigated in this work. This suggests disengagement of the two instabilities for sufficiently large times. We point out that the choice $l = 1$ filters out the possible instability of the Rossby lee wave.

An important point of observation which we shall return to later is that the growth of the $O(\epsilon)$ field is a consequence of the potential vorticity source G provided $\hat{G}(0) \neq 0$ and is not a consequence of the topography, although a weaker growth in the case of topography is not ruled out. This is why we have chosen to study explicitly the stability properties of a stationary field excited both by a potential vorticity source and by a topography.

The above considerations imply that when $\epsilon t^{\frac{2}{3}} = O(1)$ and $r = O(\epsilon^{\frac{2}{3}})$ the perturbation expansion collapses, (26) is not reliable and we need to devise another expansion which is uniformly bounded in time for $t = O(\epsilon^{-\frac{2}{3}})$. We consider again equations (10) and (11) which can be written as

$$\hat{U}_t + i\Omega(k)\,\hat{U} + r\hat{U} = -\frac{\epsilon i}{(k^2+1)}\frac{1}{(2\pi)^{\frac{1}{2}}}\int_{-\infty}^{\infty} dk'\, Z(k,k')\,\hat{V}(k',t), \tag{27}$$

$$\hat{V}_t + i\Omega(k)\,\hat{V} + r\hat{V} = \frac{\epsilon i}{(k^2+1)}\frac{1}{(2\pi)^{\frac{1}{2}}}\int_{-\infty}^{\infty} dk'\, Z(k,k')\,\hat{U}(k',t), \tag{28}$$

where $\beta = 1$ and $l = 1$ corresponding to the most dangerous meridional wavenumber from our earlier discussions. The stationary field is generated now only by the potential vorticity source $G(x)$.

From the considerations leading to the asymptotic form of the $O(\epsilon)$ field it follows that the Riemann–Lebesgue lemma cannot be invoked for a bandwidth Δk of $O(t^{-\frac{1}{3}})$

in the vicinity of $k = 0$. The failure of the perturbation expansion for $\epsilon t^{\frac{3}{2}} = O(1)$ implies that the width of the band Δk for which the response is not oscillatory is $O(\epsilon^{\frac{1}{2}})$. We conclude that the right-hand side of equations (27)–(28) can at the most yield an $O(\epsilon^{\frac{3}{2}})$ effective reinforcement mechanism which is possible only for a wave band Δk of $O(\epsilon^{\frac{1}{2}})$ in the vicinity of $k = 0$.

The arguments presented above suggest solutions of the form

$$\hat{U} = \hat{U}(t, \tau, K), \quad \hat{V} = \hat{V}(t, \tau, K), \tag{29}$$

where

$$\tau = \epsilon^{\frac{3}{2}} t, \quad K = k/\epsilon^{\frac{1}{2}}. \tag{30}$$

One of the consequences of the $O(\epsilon^{\frac{1}{2}})$ wave band involved is a slow $O(\epsilon^{-\frac{1}{2}})$ x-modulation of the perturbation field.

The equations for $\hat{U}$ and $\hat{V}$ to $O(\epsilon^{\frac{3}{2}})$ are obtained by substituting (29) and (30) into (27) and (28). It follows that

$$\hat{U}_t = \epsilon^{\frac{3}{2}} \left[-\left(\frac{r}{\epsilon^{\frac{3}{2}}} + iK^3\right) \hat{U} - \hat{U}_\tau + \frac{\hat{G}(0)}{(2\pi)^{\frac{1}{2}}} \int_{-\infty}^{\infty} dK' \, \hat{V}(t, \tau, K') \right] + O(\epsilon^{\frac{5}{2}}), \tag{31}$$

$$\hat{V}_t = \epsilon^{\frac{3}{2}} \left[-\left(\frac{r}{\epsilon^{\frac{3}{2}}} + iK^3\right) \hat{V} - \hat{V}_\tau - \frac{\hat{G}(0)}{(2\pi)^{\frac{1}{2}}} \int_{-\infty}^{\infty} dK' \, \hat{U}(t, \tau, K') \right] + O(\epsilon^{\frac{5}{2}}), \tag{32}$$

where it is required that $r = O(\epsilon^{\frac{3}{2}})$. These last two equations suggest the following formal expansion

$$\hat{U} = U_0 + \epsilon^{\frac{3}{2}} U_1 + \ldots, \quad \hat{V} = V_0 + \epsilon^{\frac{3}{2}} V_1 + \ldots. \tag{33}$$

The solution for the leading order is simply

$$U_0 = A(\tau, K), \quad V_0 = B(\tau, K). \tag{34}$$

The next order yields

$$U_{1t} = -\left(\frac{r}{\epsilon^{\frac{3}{2}}} + iK^3\right) A - A_\tau + \frac{\hat{G}(0)}{(2\pi)^{\frac{1}{2}}} \int_{-\infty}^{\infty} dK' \, B(\tau, K'), \tag{35}$$

$$V_{1t} = -\left(\frac{r}{\epsilon^{\frac{3}{2}}} + iK^3\right) B - B_\tau - \frac{\hat{G}(0)}{(2\pi)^{\frac{1}{2}}} \int_{-\infty}^{\infty} dK' \, A(\tau, K'). \tag{36}$$

The asymptotic expansion remains uniformly bounded in time for $t = O(\epsilon^{-\frac{3}{2}})$ provided the right-hand side of the last two equations is set equal to zero. This leads to the following two equations governing the long time evolution of A and B,

$$A_\tau + \left(\frac{r}{\epsilon^{\frac{3}{2}}} + iK^3\right) A = \frac{\hat{G}(0)}{(2\pi)^{\frac{1}{2}}} \int_{-\infty}^{\infty} dK' \, B(\tau, K'), \tag{37}$$

$$B_\tau + \left(\frac{r}{\epsilon^{\frac{3}{2}}} + iK^3\right) B = -\frac{\hat{G}(0)}{(2\pi)^{\frac{1}{2}}} \int_{-\infty}^{\infty} dK' \, A(\tau, K'), \tag{38}$$

rendering equations (35) and (36) homogeneous. The leading order is now affected by the nonhomogeneity of the basic field (compare with (14)) and our objective is to solve (37) and (38). Note that (37) and (38) could not have been obtained by a simple low-wavenumber approximation since in the limit $\epsilon \to 0$ the integrals that appear in these two equations should be interpreted as δ functions in the physical space (see § 4). This implies (i) that although the dominant contribution comes from the low-wave-

number components all the spectrum is in fact participating in the dynamics, (ii) that the interaction of the perturbation with the basic field takes place in a localized region of the physical space. We now define

$$M(\tau) = \int_{-\infty}^{\infty} dK' A(\tau, K'), \quad N(\tau) = \int_{-\infty}^{\infty} dK' B(\tau, K'), \tag{39}$$

so that (37) and (38) can be written as

$$A_\tau + \theta A = CN(\tau), \quad B_\tau + \theta B = -CM(\tau) \tag{40), (41}$$

with

$$\theta = \left(\frac{r}{\epsilon^{\frac{3}{2}}} + iK^3\right), \quad C = \hat{G}(0)/(2\pi)^{\frac{1}{2}}. \tag{42}$$

Equations (40) and (41) can be integrated with respect to τ to yield

$$A(\tau, K) = C e^{-\theta\tau} \int_0^\tau ds\, e^{\theta s} N(s) + A(0, K), \tag{43}$$

$$B(\tau, K) = -C e^{-\theta\tau} \int_0^\tau ds\, e^{\theta s} M(s) + B(0, K). \tag{44}$$

Integration of (43) and (44) with respect to K leads to two integral equations of the Volterra type which govern the evolution of $M(\tau)$ and $N(\tau)$. We obtain

$$M(\tau) = C \int_0^\tau ds\, N(s) \exp\left[-(\tau - s)\, r/\epsilon^{\frac{3}{2}}\right] \int_{-\infty}^{\infty} dK' \exp\left[-iK'^3(\tau - s)\right] + M(0), \tag{45}$$

$$N(\tau) = -C \int_0^\tau ds\, M(s) \exp\left[-(\tau - s)\, r/\epsilon^{\frac{3}{2}}\right] \int_{-\infty}^{\infty} dK' \exp\left[-iK'^3(\tau - s)\right] + N(0), \tag{46}$$

with

$$\int_{-\infty}^{\infty} dK' \exp\left[-iK'^3(\tau - s)\right] = 3^{-\frac{1}{2}} \Gamma(\tfrac{1}{3})\, (\tau - s)^{-\frac{1}{3}} \tag{47}$$

(see (24)). Equations (45) and (46) can be handled most effectively with the aid of the Laplace transform

$$\bar{f}(p) = \int_0^\infty dp\, e^{-pt} f(t), \tag{48}$$

and we obtain the following two algebraic equations

$$\bar{M}(p) - C \frac{\Gamma(\frac{1}{3})}{3^{\frac{1}{2}}} \left[\overline{\frac{\exp - r\tau/\epsilon^{\frac{3}{2}}}{\tau^{\frac{1}{3}}}}\right] \bar{N}(p) = \frac{1}{p} M(0), \tag{49}$$

$$\bar{N}(p) + C \frac{\Gamma(\frac{1}{3})}{3^{\frac{1}{2}}} \left[\overline{\frac{\exp - r\tau/\epsilon^{\frac{3}{2}}}{\tau^{\frac{1}{3}}}}\right] \bar{M}(p) = \frac{1}{p} N(0), \tag{50}$$

with

$$\left[\overline{\frac{\exp - r\tau/\epsilon^{\frac{3}{2}}}{\tau^{\frac{1}{3}}}}\right] = \Gamma(\tfrac{2}{3})/(p + r/\epsilon^{\frac{3}{2}})^{\frac{2}{3}}, \tag{51}$$

from Erdélyi *et al.* (1954). $M(0)$ and $N(0)$ measure the initial integrated spectrum of the disturbance. Solving (49) and (50) for $\bar{M}(p)$ and $\bar{N}(p)$ and using the inverse Laplace transform, we find that

$$\begin{pmatrix} M(\tau) \\ N(\tau) \end{pmatrix} = \frac{1}{2\pi i} \int_{c-i\infty}^{c+i\infty} dp\, \frac{e^{p\tau}(p + r/\epsilon^{\frac{3}{2}})^{\frac{2}{3}}}{p[(p + r/\epsilon^{\frac{3}{2}})^{\frac{4}{3}} + \hat{G}^2(0)\, H^2]} \begin{pmatrix} (p + r/\epsilon^{\frac{3}{2}})^{\frac{2}{3}} M(0) + \hat{G}(0)\, HN(0) \\ (p + r/\epsilon^{\frac{3}{2}})^{\frac{2}{3}} N(0) - \hat{G}(0)\, HM(0) \end{pmatrix}, \tag{52}$$

with

$$H = \Gamma(\tfrac{1}{3})\,\Gamma(\tfrac{2}{3})/3^{\frac{1}{2}}(2\pi)^{\frac{1}{2}} = (2\pi)^{\frac{1}{2}}/3 \simeq 0{\cdot}8355, \tag{53}$$

and the contour of integration in (52) is such that c is to the right of all the singular points of the integrand.

The poles and branch points of the integrand of (52) determine the time evolution of M and N which for large time is dominated by those poles having the largest real part. The poles of the integrand are located at

$$\begin{aligned} p &= 0, \\ p &= -r/\epsilon^{\frac{3}{2}} + \frac{2^{\frac{1}{2}}}{2}(1 \pm i)\,(\hat{G}(0)\,H)^{\frac{3}{2}}, \\ p &= -r/\epsilon^{\frac{3}{2}} + \frac{2^{\frac{1}{2}}}{2}(-1 \pm i)\,(\hat{G}(0)\,H)^{\frac{3}{2}}. \end{aligned} \tag{54}$$

(If $\hat{G}(0) < 0$ replace $\hat{G}(0)$ by $|\hat{G}(0)|$ in (54) and in the subsequent equations.) It is clear that exponential growth in time or instability is obtained if

$$\nu = -\frac{r}{\epsilon^{\frac{3}{2}}} + \frac{2^{\frac{1}{2}}}{2}(\hat{G}(0)\,H)^{\frac{3}{2}} > 0, \tag{55}$$

or

$$\epsilon > 2^{\frac{1}{3}} r^{\frac{2}{3}}/(\hat{G}(0)\,H) \simeq 1{\cdot}5079 r^{\frac{2}{3}}/\hat{G}(0). \tag{56}$$

Furthermore, the flow is always unstable if $r \to 0$. ν is the long time growth rate. In terms of the short time t the growth rate is given by $\epsilon^{\frac{3}{2}}\nu$.

In the case of instability the evolution of M and N is dominated by those poles with $Re\,p > 0$. We then find that

$$\begin{pmatrix} M(\tau) \\ N(\tau) \end{pmatrix} \sim R\,e^{\nu\tau} \begin{pmatrix} \cos(\xi\tau + \alpha) \\ \sin(\xi\tau + \alpha) \end{pmatrix}, \tag{57}$$

with

$$R = \frac{3(\hat{G}(0)\,H)^{\frac{3}{2}}\,(M^2(0) + N^2(0))^{\frac{1}{2}}}{2[(r/\epsilon^{\frac{3}{2}})^2 - 2^{\frac{1}{2}}(\hat{G}(0)\,H)^{\frac{3}{2}}\,(r/\epsilon^{\frac{3}{2}}) + (\hat{G}(0)\,H)^3]^{\frac{1}{2}}}, \tag{58}$$

$$\alpha = \arctan(\xi/((r/\epsilon^{\frac{3}{2}}) - \xi)) + \tan^{-1}(N(0)/M(0)) + \tfrac{1}{4}\pi, \tag{59}$$

$$\xi = \frac{2^{\frac{1}{2}}}{2}[\hat{G}(0)\,H]^{\frac{3}{2}}.$$

To obtain the spatial structure of the disturbance we substitute (57) into (43) and (44) and obtain

$$\begin{pmatrix} A(\tau, K) \\ B(\tau, K) \end{pmatrix} \sim \frac{\frac{1}{2}CRe^{\nu\tau}\exp(i(\xi\tau + \alpha))}{\xi(1+i) + iK^3} \begin{pmatrix} -i \\ -1 \end{pmatrix} + \frac{\frac{1}{2}CRe^{\nu\tau}\exp(-i(\xi\tau + \alpha))}{\xi(1-i) + iK^3} \begin{pmatrix} i \\ -1 \end{pmatrix}. \tag{60}$$

Note that the denominator of (60) is the only expression containing the spatial structure which is obtained by calculating the inverse Fourier transform of (60). We then have to evaluate the integrals

$$\frac{1}{(2\pi)^{\frac{1}{2}}} \int_{-\infty}^{\infty} dK \frac{e^{iKX}}{\xi(1 \pm i) + iK^3}, \tag{61}$$

where $X = \epsilon^{\frac{1}{2}} x$. This is accomplished most easily using contour integration and we

shall not pursue this matter any further. Equations (60) and (61) show that the x-structure of the instability consists of exponentially decaying oscillations with a wavenumber and a spatial decay rate both of $O([\hat{G}(0)\epsilon]^{\frac{1}{2}})$. We note that friction does not affect the spatial structure of the instability in spite of the fact that it does affect its growth rate in time.

The analysis presented above shows that the condition for instability is derived from the solution for M and N. In the physical space M and N are proportional to $U(0,t)$ and $V(0,t)$ (see (7)). It follows that (52) determines the evolution of the disturbance at the origin. An interesting point is that although the initial spectral distribution, i.e. $A(0,K)$ and $B(0,K)$, is sufficient to determine, using (37) and (38), the evolution of the disturbance, no instability is possible if $U(0,\tau)$ and $V(0,\tau)$ or equivalently if $M(\tau)$ and $N(\tau)$ are zero initially as evident from (57) and (58).

Equations (37) and (38) describe the evolution of the instability in terms of the stretched variables K and τ. When expressed in terms of the original variables the right-hand side of these equations contains ϵ as a multiplicative factor. The result (26) can be recovered from such equations provided the asymptotic series (13) is used again. However, the algebraic growth suggested by (26) cannot be recovered from the solution of (37) and (38) when expressed in terms of the original variables. This is a reflection of the singular nature of the problem where $\epsilon \equiv 0$ and $\epsilon \to 0$ lead to two different dynamic evolutions of the system even initially.

3. Discussion of the asymptotic results

In the preceding section we have investigated the stability properties of a steady finite-amplitude field induced by a localized topography and a localized source of potential vorticity which depend only on the zonal direction but are otherwise general. Under this constraint the basic state is governed by a linear equation which can be easily solved in the wavenumber space. In fact, the projection on zero zonal wavenumber of the advection of the perturbation vorticity by the meridional velocity of the basic state is the only information that is pertinent to the stability problem. This projection is proportional to $\hat{G}(0)$ and hence it is also proportional to the integrated strength of the forcing in the physical space. The topography is x-differentiated in the vorticity equation and as such it acts like a dipole whose integrated strength is zero. This is the reason for the stability, to the order considered, of the field induced by topographic forcing. Heat sources, on the other hand, are frequently modelled in barotropic flows by vorticity sources whose integrated strength is not zero ($\hat{G}(0) \neq 0$). Such modelling can represent the barotropic contribution to the circulation of local surface temperature anomalies which are occasionally observed in weather maps.

If the one-dimensional potential vorticity source has non-zero integrated strength, i.e. $\hat{G}(0) \neq 0$, the projection on zero zonal wavenumber of the meridional advection of the perturbation vorticity by the basic state is also different from zero. Our results demonstrate that such a basic state can become unstable depending on the relation between nonlinearity and friction and in the limit of zero friction it is always unstable.

The instability that develops is essentially a Rossby wave packet which must have zero group velocity relative to the stationary forcing for otherwise its energy will be radiated to infinity without any chance for local amplitude build-up. In fact, this is

the reason for the spatial decay of the instability which is also friction independent. The growth rate of the instability does depend, of course, on friction.

The spatial structure of the instability is slowly modulating both in space and in time. The time scale of modulation is $O(\epsilon^{-\frac{3}{2}})$. The length scale of modulation is $O(\epsilon^{-\frac{1}{2}})$. This implies that the first effect of increasing the nonlinearity is to render an instability field which is more localized in space.

The meridional wavenumber of the instability is that of a stationary Rossby wave. This is a consequence of the dynamics which selects the mode of instability with the least chance of leaking its energy to infinity.† It follows that the instability possesses a current-like structure which explains why the projection of the basic state on zero zonal wavenumber is the only information that is pertinent to the stability problem.

Our analysis indicates that the instability is a zero group-velocity phenomenon associated with a band of wavenumbers in the vicinity of $k = 0$. It is important to determine whether it is related to the Rossby wave instability of Lorenz (1972) and Gill (1974*a*). Consider first the Rossby lee wave. If it were a free-wave solution extending over all space it could not become unstable to the perturbation *considered here*. The reason follows from Fjörtoft's (1953) theorem which requires as a necessary condition for instability a perturbation possessing at least one wavelength exceeding that of the Rossby wave. In our case $l = 1$, implying that $k^2 + l^2 > 1$, and Rossby wave instability is ruled out since the wavenumber of the Rossby lee wave is one.

It remains to be seen whether this conclusion is altered by the fact that we are actually dealing with a lee wave, i.e. a forced-wave rather than with a free-wave solution. Since the projection on zero zonal wavenumber of the meridional velocity of the basic state is the only information associated with the basic state that is pertinent directly to the stability problem, it is mandatory that we should determine the contribution of the Rossby lee wave to this projection. We shall do this through an illustration.

Consider the 'top-hat' potential vorticity source.

$$G = \begin{cases} 0, & x < 0, \\ 1, & 0 < x < L_0, \\ 0, & x > L_0, \end{cases} \tag{62}$$

with

$$\hat{G}(0) = L_0/(2\pi)^{\frac{1}{2}}. \tag{63}$$

In the absence of friction the basic state is governed by

$$\phi_{xxx} + \phi_x = G \tag{64}$$

with

$$\hat{\phi}_x = \hat{G}(k)/(1-k^2), \quad \hat{\phi}_x(0) = \hat{G}(0) = L_0/(2\pi)^{\frac{1}{2}}. \tag{65}$$

The solution for the meridional velocity is given by

$$\phi_x = \begin{cases} 0, & x < 0, \\ 1 - \cos x, & 0 < x < L_0, \\ \cos(x - L_0) - \cos x, & x > L_0. \end{cases} \tag{66}$$

† This statement is open to criticism if the resonant instability of the Rossby lee wave does exist.

Here, $1-\cos x$ is the local field and $\cos(x-L_0)-\cos x$ is the solution for the Rossby lee wave. It follows that the projection of the local field on $k=0$ is given by

$$\hat{\phi}_x^l(0) = \frac{1}{(2\pi)^{\frac{1}{2}}}(L_0 - \sin L_0), \tag{67}$$

implying that the corresponding projection of the Rossby lee wave is

$$\hat{\phi}_x^R(0) = \frac{1}{(2\pi)^{\frac{1}{2}}}\sin L_0. \tag{68}$$

We conclude that the Rossby lee wave contributes to $\hat{\phi}_x(0)$ and hence it is responsible in part for the instability; nevertheless it is not essential for the instability. In fact, if $L_0 = n\pi$ and n is an integer $\hat{\phi}_x^R(0) = 0$ and the local field is the sole contributor to the instability. Furthermore, if n is even the Rossby lee wave vanishes altogether and the local field is the only non-trivial solution. This example demonstrates that the source of the instability is the local field and that it is not at all related to the familiar Rossby wave instability. This point has been verified by numerical integration of the initial-value problem for finite ϵ.

Figure 2 depicts the meridional velocity of the basic state (66) for $L_0 = 1$. The stream function of the total basic field (zonal flow plus the field induced by the potential vorticity source) is given by $-y+\epsilon\phi$. Streamlines of this field for $\epsilon = 6$ and the potential vorticity source (62) are shown in figure 3. This is a case of strong streamwise nonhomogeneity for which numerical results are presented in the next section.

The above example besides emphasizing the important role of $\hat{G}(0)$ shows also that $\hat{G}(0) = O(L_s/(U^*/\beta')^{\frac{1}{2}})$, where L_s is a typical length scale of the source (for the 'top-hat' profile $L_0 = L_s/(U^*/\beta')^{\frac{1}{2}}$). This implies that the instability mechanism can be efficient only for potential vorticity sources whose typical length scale is equal to or larger than the scale of the stationary Rossby wave. Mid-latitude atmospheric conditions yield $(U^*/\beta')^{\frac{1}{2}} \simeq 750$ km.

The important role of the meridional velocity of the basic state emerges also from energy considerations. Consider, for simplicity, the case of $F=0$, $l=1$, $\beta=1$ and $r=0$. Multiply (8) by U, (9) by V and use (2) to eliminate ϕ_{xxx}. Combine the two equations and integrate the resulting equation over x to yield the following energy integral of the perturbation field

$$\begin{aligned}\frac{d}{dt}\int_{-\infty}^{\infty} \tfrac{1}{2}(U_x^2+U^2+V_x^2+V^2)\,dx &= \epsilon\int_{-\infty}^{\infty}\phi_x(VU_{xx}-UV_{xx})\,dx \\ &= \epsilon\int_{-\infty}^{\infty}(UV_x-VU_x)\,\phi_{xx}\,dx.\end{aligned} \tag{69}$$

We observe that instability is possible provided the Reynolds stress induced by the meridional velocity of the basic state and the zonal velocity of the perturbation field is positively correlated with the vorticity of the perturbation field, or equivalently that the meridionally averaged Reynolds stress field of the perturbation is positively correlated with the vorticity of the basic field.

We have investigated the leading order of the linear phase of the evolution of the instability for small ϵ and have found out that the growth rate is exponential. It is clear that the analysis must be modified for $t > O(\epsilon^{-\frac{3}{2}})$. Equations (35) and (36) suggest

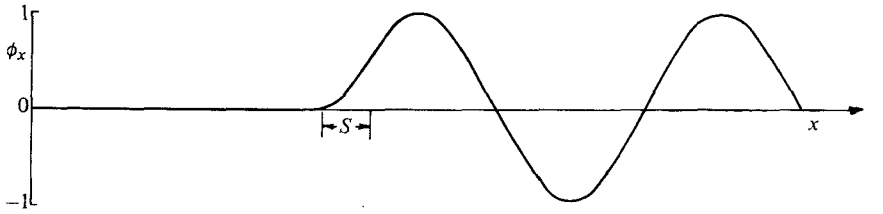

FIGURE 2. The meridional velocity of the basic state, as given by (66) for $L_0 = 1$. The location of the potential vorticity source is denoted by S. $L_0 = 1$ corresponds to 750 km for mid-latitude atmospheric conditions.

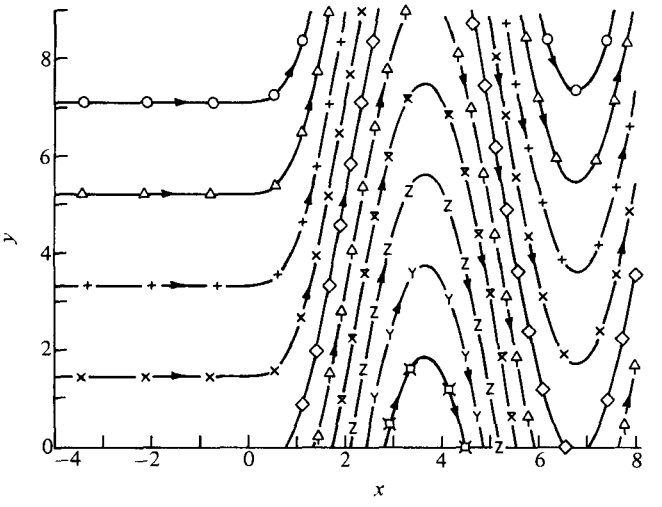

FIGURE 3. Streamlines of the unperturbed field which consists of a uniform zonal flow plus a deviation induced by the potential vorticity source (62) for $\epsilon = 6$. The 'top-hat' potential vorticity source stretches from $x = 0$ to $x = 1$. The origin of the y-co-ordinate is arbitrary. The arrows indicate the direction of the flow and we observe a pure zonal flow ahead of the forcing and a meandering flow downstream of it. ○, −1·7138; △, 0·1724; +, 2·0586; ×, 3·9448; ◇, 5·8310; ⏢, 7·7171; ⧖, 9·6033; Z, 11·4895; Y, 13·3757; ⧈, 15·2619.

that there is no $O(\epsilon^{\frac{3}{2}})$ correction, since if we exclude the possibility of modifying the y-structure, U_1 and V_1 must be functions of τ and K only and consequently can be absorbed in the leading order. It follows that the next correction to the linear problem is $O(\epsilon^{\frac{5}{2}})$. This indicates that nonlinear effects should probably be considered before the instability cascades down the spectrum. The extension of the asymptotic study into the nonlinear region is a formidable task and it is difficult, at this stage, to predict the final state of the system. We can only be guided by the results of the linear analysis and speculate that the system will evolve into an effectively new steady state which, however, may modulate slowly in time. If this is the case then the system will move through an instability mechanism from one steady state to another once the conditions for instability are met. This is in line with the work of Charney & Devore (1979) although the evolution here is entirely local. If the qualitative appearance of the instability does not change much in the nonlinear regime then its meridional structure when superimposed on the basic field should produce in the Rossby lee wave region, i.e. downstream of the potential vorticity source, large meridional excursions from zonal flow. This situation is referred to as blocking in meteorology. This conclusion is in agreement with Merkine (1980). Note that the nonlinear analysis should include the

quadratic terms of the perturbation field that were neglected in (6) and the back effect of the perturbation field on the zonal flow which provides the mechanism for changing the basic field ϕ.

4. Numerical solution for finite ϵ

The asymptotic analysis of the previous sections is supplemented in this section by some numerical examples. We consider the case of $l = 1$, $\beta = 1$, $r = 0$ and $F = 0$. Equations (8) and (9) can be written as

$$\begin{aligned} \zeta_t &= -(\zeta + U)_x + \epsilon\phi_x(\eta + V) - \epsilon GV, \\ \eta_t &= -(\eta + V)_x - \epsilon\phi_x(\zeta + U) + \epsilon GU, \end{aligned} \tag{70}$$

where

$$\zeta = U_{xx} - U, \quad \eta = V_{xx} - V \tag{71}$$

are the vorticity components of the disturbance. The vorticity source is given by (62) and ϕ_x by (66). Equations (70) and (71) are supplemented by the initial condition

$$t = 0, \quad U = \exp(-a(x-b)^2), \quad V = 0, \tag{72}$$

where a and b are constants determining the steepness and the location of the initial pulse. Physically, the initial disturbance can be viewed as an eddy advected downstream by the westerly flow or generated locally by baroclinic activity, for instance.

In the absence of forcing, i.e. when $\epsilon = 0$, the initial disturbance consists of a group of Rossby waves dispersing with time. No wave energy can propagate upstream since the group velocity given by

$$d\Omega/dk = k^2(3 + k^2)/(1 + k^2)^2 \tag{73}$$

is always positive. For an initial concentrated disturbance released at $x = 0$ the region occupied by waves is

$$0 \leqslant x/t \leqslant \tfrac{9}{8}, \tag{74}$$

where the long waves are found near the tail of the wave packet and their amplitude decays at a rate $t^{-\frac{1}{2}}$. The front of the wave train consists of waves with wavenumbers $k \simeq 3^{\frac{1}{2}}$ whose decay rate is again $t^{-\frac{1}{2}}$. Outside these two caustic regions the decay rate of the wave packet is $t^{-\frac{1}{2}}$.

The physical boundary conditions require vanishing of the disturbance at large distances from its region of excitation. Thus, as long as the domain of integration is sufficiently large, such boundary conditions can indeed be satisfied. The actual domain of integration extended from $x = -10$ to $x = 17$, implying that the region (74) starts interacting with the boundary at $t \simeq 15$. The boundary conditions used were

$$\begin{aligned} x &= -10, \quad U = V = \zeta = \eta = 0, \\ x &= 17, \quad U = V = \zeta_{xx} = \eta_{xx} = 0. \end{aligned} \tag{75}$$

The conditions imposed on the vorticity at $x = 17$ amount to extrapolating the vorticity outward. It allows the wave packet to leave the domain of integration at the price of a local distortion of the solution in the immediate vicinity of $x = 17$. This permits us to extend the time integration beyond $t = 15$. Centred space derivatives were used with $\Delta x = 0{\cdot}2$. The integration in time was advanced using Lorenz's N-cycle scheme with $N = 4$ and the small time increment was set equal to 0·025

satisfying CFL stability condition. (The phase speed of the waves is less than 1.) The new values of U and V were obtained after each time increment from the updated vorticity (71) by inverting a tri-diagonal matrix using the double-sweep method. The numerical scheme was checked for the case of $\epsilon = 0$ for which the evolution of the wave packet is known. It worked satisfactorily; in particular, the decay rate of the amplitude of the long waves was $t^{0.31}$.

Difficulties may occur when ϵ is finite since the numerical scheme may not properly resolve the region of energy extraction with the consequence of underestimating the actual strength of the phenomenon. To illustrate the point we now derive in a direct way the asymptotic limit of equations (70) for $\epsilon \to 0$ without transforming the equations into the spectral domain. We introduce the scaling

$$X = \epsilon^{\frac{1}{2}} x, \quad \tau = \epsilon^{\frac{3}{2}} t \tag{76}$$

into (70) and obtain that

$$\begin{aligned} \epsilon^{\frac{3}{2}}(\epsilon U_{XX\tau} - U_\tau + U_{XXX}) &= \epsilon(\epsilon\phi_x(X/\epsilon^{\frac{1}{2}})\, V_{XX} - G(X/\epsilon^{\frac{1}{2}})\, V), \\ \epsilon^{\frac{3}{2}}(\epsilon V_{XX} - V_\tau + V_{XXX}) &= -\epsilon(\epsilon\phi_x(X/\epsilon^{\frac{1}{2}})\, U_{XX} - G(X/\epsilon^{\frac{1}{2}})\, U). \end{aligned} \tag{77}$$

Observing that

$$G(X/\epsilon^{\frac{1}{2}}) = \begin{cases} 0, & |X| = O(1), \\ O(1), & |X| = O(\epsilon^{\frac{1}{2}}), \end{cases} \tag{78}$$

$$\phi_x(X/\epsilon^{\frac{1}{2}}) = \begin{cases} 0, & X < 0, \\ O(1), & X > 0, \end{cases} \tag{79}$$

for small ϵ, we find that in the limit of $\epsilon \to 0$ equations (77) become

$$\begin{aligned} U_\tau - U_{XXX} &= \mu\delta(X)\, V, \quad \mu = \int_{-\infty}^{\infty} dx\, G(x) = (2\pi)^{\frac{1}{2}}\, \hat{G}(0), \\ V_\tau - V_{XXX} &= -\mu\delta(X)\, U, \end{aligned} \tag{80}$$

where $\delta(X)$ is the Dirac delta function.

The numerical difficulties are obvious. The energy extraction from the mean flow takes place in a very narrow zone compared to the length scale of the instability. For small ϵ the width of this zone is $O(\epsilon^{\frac{1}{2}})$ relative to the scale of X, and it is not obvious how it increases with ϵ. This may be the reason for the relatively little success of general circulation models in simulating or predicting blocking configurations. Although such models can adequately resolve the blocking length scale they are incapable of resolving the crucial energy extraction zone.

The same difficulty seemed to occur in the numerical integration of equations (70) with the prescribed spatial resolution. The results presented are for $\epsilon = 6$ and the integration was carried out to $t = 15$. For smaller values of ϵ the integration had to be extended well beyond this value of t in order to observe the evolution of the instability. The numerical results verified all the qualitative predictions of the asymptotic analysis. However, the limitations of the numerical scheme for small ϵ (long integrations and the finiteness of the domain) precludes the possibility of direct comparison of the results with the asymptotic study.

Figures 4–11 depict the results of the numerical integration for $L_0 = 1$ (see (62) and (66)), $a = 1$ and $b = \frac{1}{2}$ (see (72)). We observe the rapid evolution of a nonpropagating

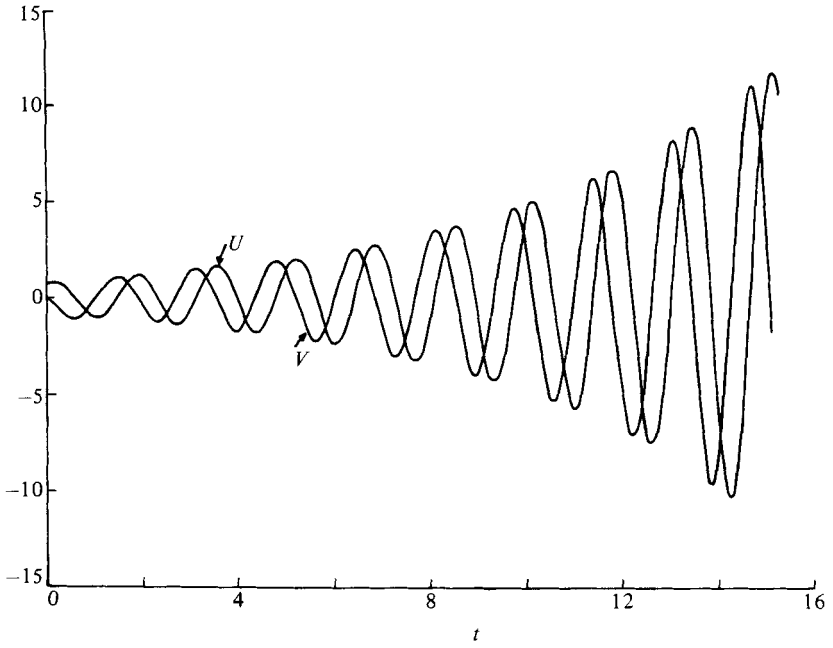

FIGURE 4. The time evolution of the instability at $x = 1$. The undisturbed field is shown in figure 3. The initial disturbance is centred in the potential vorticity source region. It has a Gaussian shape with a length scale comparable to that of the forcing.

wave packet whose growth in time is exponential with a growth rate of 0·174. This corresponds to an e-folding time of 5 days for $U^* = 10$ m/sec and $L = (U^*/\beta')^{\frac{1}{2}} = 750$ km. Although the wave packet is not propagating in the x-direction it is oscillatory. This oscillation in combination with the periodicity in y allows phase-velocity propagation in the y-direction. Figure 4 shows the time evolution of the instability at $x = 1$ which is the approximate location where the U and V fields attain their maximal values. The period of oscillation is 1·650 or 1·43 days for the same values of U^* and L. The frequency of oscillation is 3·81. Other numerical integrations indicate that both the growth rate and the frequency increase with ϵ in agreement with the overall predictions of the asymptotic results. However, we cannot infer from these numerical results that a transition to a new quasi-steady flow is in fact taking place since the instability is highly oscillatory.

An estimate of the scale of the packet is somewhat arbitrary but it is fair to say that it is close to that of a stationary Rossby wave. This implies that the spectrum of the packet is dominated by wavenumbers lower than $(\beta'/U^*)^{\frac{1}{2}}$. Therefore, another qualitative prediction of the asymptotic analysis is verified: an increase in ϵ results in narrower packets. An important consequence of the shrinking of the zonal scale of the packet for large ϵ is that the meridional velocity of the perturbation becomes comparable to the zonal velocity of the perturbation. Large meridional velocity implies large meridional displacements of streamlines with the flow field assuming, in the x-direction, the form of a non-propagating meandering flow. It should be remembered that the perturbation field is linear and is determined up to a multiplicative constant. Hence the full impact of the instability on the flow field cannot be assessed until nonlinear effects are brought into consideration.

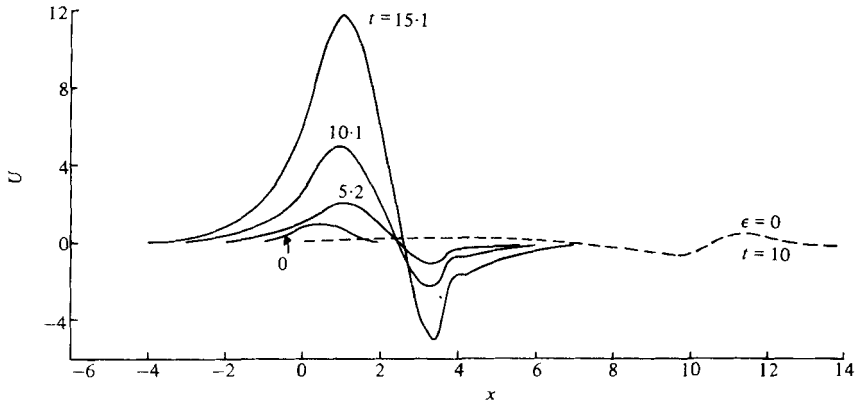

FIGURE 5. The U field of the unstable wave packet at times $t = 5{\cdot}2$, $10{\cdot}1$ and $15{\cdot}1$. The undisturbed field is shown in figure 3. $t = 0$ denotes the initial disturbance. The dashed line denotes the fate of the disturbance at $t = 10$ corresponding to the case of no forcing, i.e. $\epsilon = 0$.

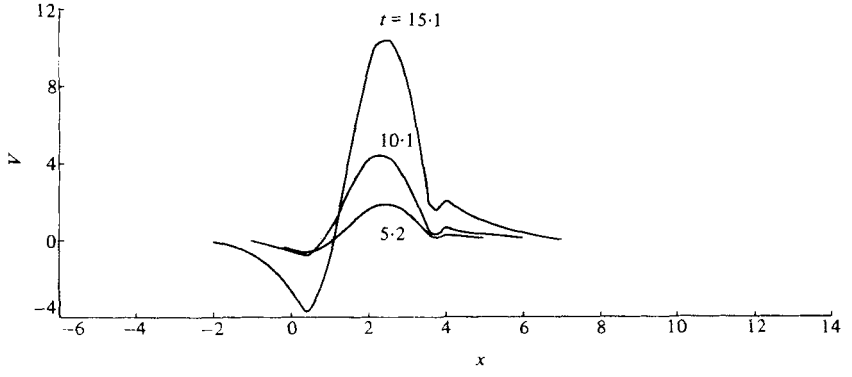

FIGURE 6. The V field of the unstable wave packet at times $t = 5{\cdot}2$, $10{\cdot}1$ and $15{\cdot}1$ corresponding to the conditions of figure 5. $V = 0$ at $t = 0$.

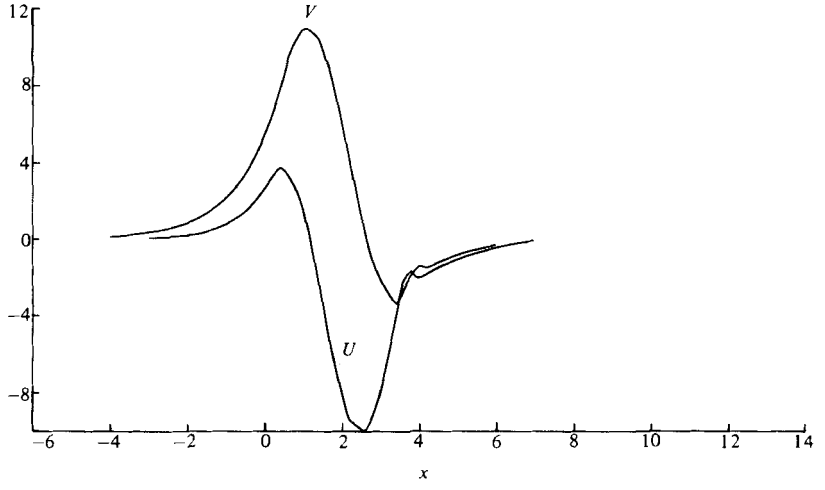

FIGURE 7. The U and V fields of the unstable wave packet at $t = 14{\cdot}7$ corresponding to the conditions of figure 5. $t = 14{\cdot}7$ is approximately a quarter of a cycle earlier than $t = 15{\cdot}1$.

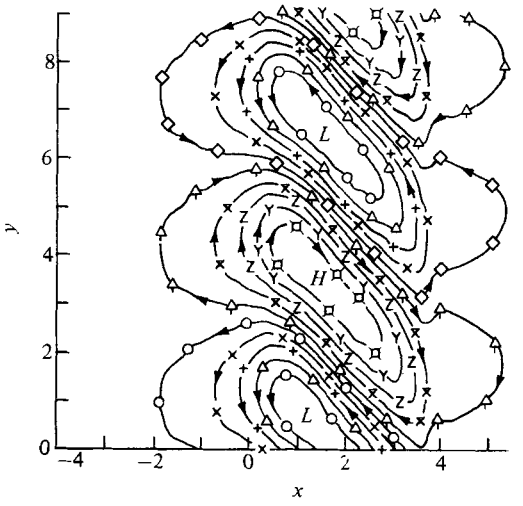

FIGURE 8. Streamlines of the instability field $U(x, t) \sin y + V(x, t) \cos y$ at $t = 14{\cdot}3$. The arrows indicate the direction of the circulation. Counter-clockwise circulations are centred around regions of low perturbation pressure denoted by L. Clockwise circulations are centred around regions of high perturbation pressure denoted by H. The origin of the y-co-ordinate is arbitrary. The corresponding unperturbed field is shown in figure 3. In figures 8–11 the amplitude of the initial perturbation is ten times smaller than that of figures 4–7. ○, −0·8547; △, −0·6647; +, −0·4746; ×, −0·2846; ◇, −0·0946; △, 0·0955; ⧖, 0·2855; **Z**, 0·4755; **Y**, 0·6656; ⌑, 0·8556.

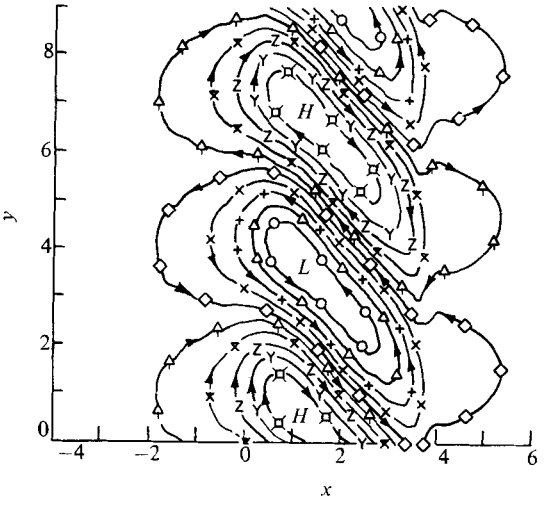

FIGURE 9. Same as in figure 8 but approximately half a period of oscillations later, $t = 15{\cdot}1$. ○, −0·9634; △, −0·7489; +, −0·5344; ×, −0·3200; ◇, −0·1055; △, 0·1090; ⧖, 0·3234; **Z**, 0·5379; **Y**, 0·7524; ⌑, 0·9668.

Figures 5 and 6 depict the zonal structure of the disturbance at $t = 5{\cdot}2$, $10{\cdot}1$ and $15{\cdot}1$. At these times, which are three cycles apart (see figure 4), the oscillatory part of the U field attains its maximum. Figure 4 shows that the U and V fields are a quarter of a cycle out of phase, which is also apparent from figures 6 and 7. The U field at $t = 15{\cdot}1$ (see figure 5) has the same shape as the V field at $t = 14{\cdot}7$ (see figure 7), which is approximately a quarter of a cycle earlier. This 90° phase difference yields a

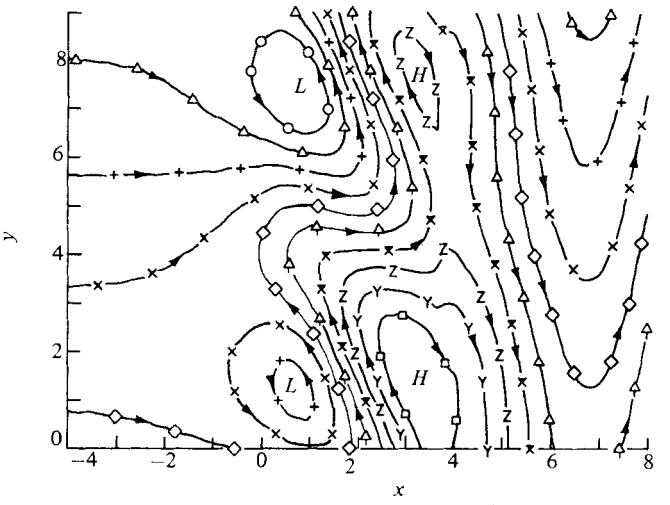

FIGURE 10. Streamlines of the basic field (figure 3) plus the instability (figure 8) at $t = 14{\cdot}3$. Flow direction is denoted by arrows. L and H correspond to low- and high-pressure regions, respectively. ○, −5·0638; △, −2·6615; +, −0·2592; ×, 2·1430; ◇, 4·5453; △, 6·9476; ⊼, 9·3499; Z, 11·7522; Y, 14·1545; ⊔, 16·5568.

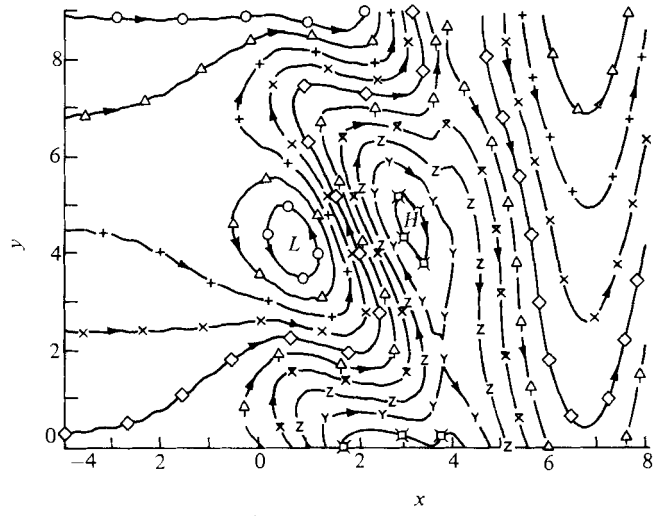

FIGURE 11. Same as in figure 10 but approximately half a period of oscillations later, $t = 15{\cdot}1$. ○, −3·5152; △, −1·3394; +, 0·8364; ×, 3·0122; ◇, 5·1880; △, 7·3638; ⊼, 9·5396; Z, 11·7154; Y, 13·8911; ⊔, 16·0669.

Reynolds stress field which is highly correlated with the vorticity of the basic field (see (69)), implying maximal energy extraction from the basic field.

Figures 8–11 depict the two-dimensional structure of the flow field where the initial field given by (72) is multiplied by 0·1. Figures 8 and 9 show the two-dimensional structure of the instability (streamlines) at times $t = 14{\cdot}3$ and $t = 15{\cdot}1$ which are approximately half a cycle apart. The stream function of the instability is given by (7). The structure which is periodic in y is localized and nonpropagating in x. The instability assumes the form of alternating closed circulations which are slanted from north-west to south-east. In the framework of the quasi-geostrophic approximation streamlines

are parallel to isobars and high/low pressure centres are associated with clockwise/counter-clockwise circulations. The zonal scale of the wave packet is similar to its meridional scale. The elongated structure of the instability implies that strong alternating jets are aligned with the direction of the cells. It follows that in the region of the instability the zonal and meridional components of the perturbation velocity are negatively correlated. Again we observe a meridionally averaged Reynolds stress field which is positively correlated with the vorticity of the basic flow, which in turn effects energy extraction from the mean flow into the perturbation.

The stream function of the total field, i.e. the basic field plus the perturbation, is given by $-y+\epsilon(\phi+\varphi)$. If $|\varphi| \ll |\phi|$ the instability can be approximated by (7). Otherwise, a superposition of the basic field plus the linear perturbation can only give a crude approximation of the actual flow behaviour, since wave–wave interactions should then be taken into consideration. Such a superposition is included here for the sake of completeness. The superposition of the streamfunctions corresponding to figures 8 and 3 and figures 9 and 3 yields the streamlines depicted in figures 10 and 11. We observe that the zonal flow is decelerated in the region where the jets of the instability are south-easterly and that it is accelerated in the region where the jets of the instability are north-westerly. In the region of zonal flow deceleration blocking configuration with closed circulation develops. Overall, the effect of the instability is confined to the region of the potential vorticity source and to some distance downstream of it.

Atmospheric blocking tends to occur at fixed geographical locations relative to the distribution of oceans and continents (Charney & Devore 1979). We have repeated the numerical integration with different initial conditions by varying a and b, i.e. changing the steepness and location of the initial disturbance, placing it upstream or downstream of the vorticity source. The instability always developed at the same location relative to the forcing and the same growth rate was obtained. We also integrated the equations for the case of $L_0 = 2\pi$ such that no lee wave is excited by the potential vorticity source (62) as evident from (66). An unstable nonpropagating wave packet developed, in agreement with the discussion of the previous section, but the growth rate obtained was considerably less than that of the example presented above.

The asymptotic analysis of the previous sections showed that, at least for weak forcing, the field induced by topography is stable. It is important to determine whether instability exists for strong topographic forcing. We have made numerical integrations for the case of topography whose shape is given by the 'top-hat' profile (62). The basic meridional velocity ϕ_x is different from that given by (66) but is obtained with the same ease. The other modification requires the elimination of the G terms from (70). Various initial conditions were considered with values of ϵ as large as 10. In agreement with the results of the asymptotic study no instability was observed.

Gill, in an unpublished manuscript (1974*b*), reported the results of a numerical experiment with a periodic two-layer model in which motion was driven by a wind stress having the largest scale and the bottom topography included a meridional ridge and scattered topographic features. Baroclinic instability occurred at wavenumber 6 in agreement with the linear theory. At later times there was a significant energy build-up at lower wavenumbers and the region of activity was that of standing lee waves in an eastward current. It was suggested that nonlinear transfer of energy

from wavenumber 6 to lower wavenumbers took place. It is also possible that resonant instability of the lee waves was triggered when the nonhomogeneity of the stationary pattern reached a sufficient degree of intensity as more energy was fed into the largest scale by the applied wind stress.

5. Baroclinic flows

In this section we generalize the asymptotic study of §2 to baroclinic flows. We consider the two-layer beta plane model for a quasi-geostrophic baroclinic flow in a horizontally open domain which is confined vertically by two horizontal planes a distance D apart. In the absence of motion the two layers are of equal depth. The flow consists of a vertically sheared horizontally uniform westerly flow U_n ($n = 1$ for the upper layer and $n = 2$ for the lower layer) plus a deviation arising from the presence of a localized potential vorticity source S_n. The non-dimensional equations governing the deviation stream function ψ_n are

$$\left(\frac{\partial}{\partial t}+(1+\tfrac{1}{2}\Delta)\frac{\partial}{\partial x}\right)(\nabla^2\psi_1+F(\psi_2-\psi_1))+(1+F\Delta)\frac{\partial\psi_1}{\partial x}+r\nabla^2\psi_1 = -\epsilon J(\psi_1,\nabla^2\psi_1+F(\psi_2-\psi_1))+S_1, \quad (81)$$

$$\left(\frac{\partial}{\partial t}+(1-\tfrac{1}{2}\Delta)\frac{\partial}{\partial x}\right)(\nabla^2\psi_2+F(\psi_1-\psi_2))+(1-F\Delta)\frac{\partial\psi_2}{\partial x}+r\nabla^2\psi_2 = -\epsilon J(\psi_2,\nabla^2\psi_2+F(\psi_1-\psi_2))+S_2, \quad (82)$$

where $U^* = \frac{1}{2}(U_1+U_2)$ is the horizontal velocity scale, $L = (U^*/\beta')^2$ is the horizontal length scale and time is scaled accordingly. $\Delta = (U_1-U_2)/U^*$ is the shear parameter and $F = L^2/L_R^2$ is the rotational Froude number, where the radius of deformation, L_R, is given by $(gD(\rho_2-\rho_1)/(2\rho_2))^{\frac{1}{2}}/f_0$. ϵ and r have the same meaning as in §2. The derivation of (81) and (82) is given by Pedlosky (1970) with somewhat different normalization.

We find it more convenient to separate barotropic and baroclinic effects. Consequently, we write

$$\psi_m = \tfrac{1}{2}(\psi_1+\psi_2), \quad \psi_\tau = \tfrac{1}{2}(\psi_1-\psi_2), \quad S_m = \tfrac{1}{2}(S_1+S_2), \quad S_\tau = \tfrac{1}{2}(S_1-S_2), \quad (83)$$

and add and subtract equations (81) and (82) to obtain

$$\left(\frac{\partial}{\partial t}+\frac{\partial}{\partial x}\right)\nabla^2\psi_m+\frac{\partial\psi_m}{\partial x}+r\nabla^2\psi_m+\tfrac{1}{2}\Delta\frac{\partial\nabla^2\psi_\tau}{\partial x} = -\epsilon J(\psi_m,\nabla^2\psi_m)-\epsilon J(\psi_\tau,\nabla^2\psi_\tau)+S_m, \quad (84)$$

$$\left(\frac{\partial}{\partial t}+\frac{\partial}{\partial x}\right)(\nabla^2\psi_\tau-2F\psi_\tau)+\frac{\partial\psi_\tau}{\partial x}+r\nabla^2\psi_\tau+\tfrac{1}{2}\Delta\frac{\partial\nabla^2\psi_m}{\partial x}+F\Delta\frac{\partial\psi_m}{\partial x} = -\epsilon J(\psi_m,\nabla^2\psi_\tau)-\epsilon J(\psi_\tau,\nabla^2\psi_m)+2F\epsilon J(\psi_m,\psi_\tau)+S_\tau. \quad (85)$$

Assume that $S_m = S_m(x)$ and $S_\tau = S_\tau(x)$ and let $(\phi_m(x), \phi_\tau(x))$ be the corresponding steady-state solution which is governed by

$$\frac{\partial^3\phi_m}{\partial x^3}+\frac{\partial\phi_m}{\partial x}+r\frac{\partial^2\phi_m}{\partial x^2}+\tfrac{1}{2}\Delta\left(\frac{\partial^3\phi_\tau}{\partial x^3}-2F\frac{\partial\phi_\tau}{\partial x}\right)+F\Delta\frac{\partial\phi_\tau}{\partial x} = S_m, \quad (86)$$

$$\frac{\partial^3\phi_\tau}{\partial x^3}-2F\frac{\partial\phi_\tau}{\partial x}+\frac{\partial\phi_\tau}{\partial x}+r\frac{\partial^2\phi_\tau}{\partial x^2}+\tfrac{1}{2}\Delta\frac{\partial^3\phi_m}{\partial x^3}+F\Delta\frac{\partial\phi_m}{\partial x} = S_\tau. \quad (87)$$

The solution of (86) and (87) satisfies exactly the nonlinear equations (84) and (85) for finite ϵ.

Let

$$\psi_m = \phi_m(x) + \varphi_m(x,y,t), \quad \psi_\tau = \phi_\tau(x) + \varphi_\tau(x,y,t), \tag{88}$$

where φ_m and φ_τ are the barotropic and baroclinic perturbations of the basic state. The linear equations governing the evolution of φ_m and φ_τ are obtained by substituting (88) into (86) and (87) and neglecting quadratic terms of the perturbation field. We obtain

$$\left(\frac{\partial}{\partial t}+\frac{\partial}{\partial x}\right)\nabla^2\varphi_m+\frac{\partial\varphi_m}{\partial x}+r\nabla^2\varphi_m+\tfrac{1}{2}\Delta\frac{\partial\nabla^2\varphi_\tau}{\partial x}$$
$$=-\epsilon\frac{\partial\phi_m}{\partial x}\frac{\partial\nabla^2\varphi_m}{\partial y}+\epsilon\frac{\partial^3\phi_m}{\partial x^3}\frac{\partial\varphi_m}{\partial y}-\epsilon\frac{\partial\phi_\tau}{\partial x}\frac{\partial\nabla^2\varphi_\tau}{\partial y}+\frac{\partial^3\phi_\tau}{\partial x^3}\frac{\partial\varphi_\tau}{\partial y}, \tag{89}$$

$$\left(\frac{\partial}{\partial t}+\frac{\partial}{\partial x}\right)(\nabla^2\varphi_\tau-2F\varphi_\tau)+\frac{\partial\varphi_\tau}{\partial x}+r\nabla^2\varphi_\tau+\tfrac{1}{2}\Delta\frac{\partial\nabla^2\varphi_m}{\partial x}+F\Delta\frac{\partial\varphi_m}{\partial x}$$
$$=-\epsilon\frac{\partial\phi_m}{\partial x}\frac{\partial\nabla^2\varphi_\tau}{\partial y}+\epsilon\frac{\partial^3\phi_\tau}{\partial x^3}\frac{\partial\varphi_m}{\partial y}-\epsilon\frac{\partial\phi_\tau}{\partial x}\frac{\partial\nabla^2\varphi_m}{\partial y}+\epsilon\frac{\partial^3\phi_m}{\partial x^3}\frac{\partial\varphi_\tau}{\partial y}+2\epsilon F\left(\frac{\partial\phi_m}{\partial x}\frac{\partial\varphi_\tau}{\partial y}-\frac{\partial\phi_\tau}{\partial x}\frac{\partial\varphi_m}{\partial y}\right). \tag{90}$$

The stability analysis is motivated by the approach described at length in §2 and for the sake of brevity we shall skip unnecessary details. We assume that the perturbation field can be written

$$\varphi_m = U_m(x,t)\sin ly + V_m(x,t)\cos ly, \quad \varphi_\tau = U_\tau(x,t)\sin ly + V_\tau(x,t)\cos ly, \tag{91}$$

and substitute (91) into (89) and (90) which are then converted into the following four integro-differential equations

$$\hat{U}_{mt}+ik\left(1-\frac{1}{k^2+l^2}\right)\hat{U}_m+r\hat{U}_m+\tfrac{1}{2}ik\Delta\hat{U}_\tau$$
$$=-\frac{\epsilon li}{(2\pi)^{\frac{1}{2}}(k^2+l^2)}\int_{-\infty}^{\infty}dk'\,[Z_m(k,k')\,\hat{V}_m(k',t)+Z_\tau(k,k')\,\hat{V}_\tau(k',t)], \tag{92}$$

$$\hat{V}_{mt}+ik\left(1-\frac{1}{k^2+l^2}\right)\hat{V}_m+r\hat{V}_m+\tfrac{1}{2}ik\Delta\hat{V}_\tau$$
$$=\frac{\epsilon li}{(2\pi)^{\frac{1}{2}}(k^2+l^2)}\int_{-\infty}^{\infty}dk'\,[Z_m(k,k')\,\hat{U}_m(k',t)+Z_\tau(k,k')\,\hat{U}_\tau(k',t)], \tag{93}$$

$$\hat{U}_{\tau t}+ik\left(1-\frac{1}{k^2+l^2+2F}\right)\hat{U}_\tau+r\frac{k^2+l^2}{k^2+l^2+2F}\hat{U}_\tau+\tfrac{1}{2}ik\Delta\frac{k^2+l^2-2F}{k^2+l^2+2F}\hat{U}_m$$
$$=-\frac{\epsilon li}{(2\pi)^{\frac{1}{2}}(k^2+l^2+2F)}\int_{-\infty}^{\infty}dk'\,[Y_m(k,k')\,\hat{V}_\tau(k',t)+Y_\tau(k,k')\,\hat{V}_m(k',t)], \tag{94}$$

$$\hat{V}_{\tau t}+ik\left(1-\frac{1}{k^2+l^2+2F}\right)\hat{V}_\tau+r\frac{k^2+l^2}{k^2+l^2+2F}\hat{V}_\tau+\tfrac{1}{2}ik\Delta\frac{k^2+l^2-2F}{k^2+l^2+2F}\hat{V}_m$$
$$=\frac{\epsilon li}{(2\pi)^{\frac{1}{2}}(k^2+l^2+2F)}\int_{-\infty}^{\infty}dk'\,[Y_m(k,k')\,\hat{U}_\tau(k',t)+Y_\tau(k,k')\,\hat{U}_m(k',t)], \tag{95}$$

where

$$\left.\begin{aligned} Z_m(k,k') &= (k-k')(k^2-2kk'-l^2)\hat{\phi}_m(k-k'),\\ Z_\tau(k,k') &= (k-k')(k^2-2kk'-l^2)\hat{\phi}_\tau(k-k'),\\ Y_m(k,k') &= (k-k')(k^2-2kk'-l^2-2F)\hat{\phi}_m(k-k'),\\ Y_\tau(k,k') &= (k-k')(k^2-2kk'-l^2+2F)\hat{\phi}_\tau(k-k'),\end{aligned}\right\} \tag{96}$$

and

$$\left.\begin{aligned} \hat{\phi}_m &= \frac{i[(k^2+2F-1-irk)\hat{S}_m-\frac{1}{2}\Delta k^2\hat{S}_\tau]}{k[(k^2-1-irk)(k^2+2F-1-irk)-\frac{1}{2}\Delta^2k^2(\frac{1}{2}k^2-F)]},\\ \hat{\phi}_\tau &= \frac{i[(k^2-1-irk)\hat{S}_\tau-\Delta(\frac{1}{2}k^2-F)\hat{S}_m]}{k[(k^2-1-irk)(k^2+2F-1-irk)-\frac{1}{2}\Delta^2k^2(\frac{1}{2}k^2-F)]}.\end{aligned}\right\} \tag{97}$$

When $\epsilon = 0$ (92)–(96) possess solutions which are proportional to $e^{-i\lambda t}$ with

$$\lambda = k - k\frac{k^2+l^2+F}{k^2+l^2+2F}\left(\frac{1}{k^2+l^2}+\frac{ir}{k}\right) \pm k\frac{[\Delta^2(k^2+l^2)^2((k^2+l^2)^2-4F^2)+4F^2(1+ir(k^2+l^2)/k)^2]^{\frac{1}{2}}}{2(k^2+l^2)(k^2+l^2+2F)}. \tag{98}$$

The expression for λ is identical with that given by equation (3.5) of Pedlosky (1970) with $\beta = 1$ as implied by our nondimensionalization. Our investigation is restricted to the case $\epsilon \ll 1$ and similarly to the barotropic case we shall find that the $O(\epsilon)$ potential vorticity source cannot significantly affect the dynamics for times which are less than $O(\epsilon^{-\frac{3}{2}})$. On a shorter time scale the flow field can be destabilized by baroclinic instability if the shear is sufficiently strong. The condition for the initiation of baroclinic instability is singular in r in the sense that the threshold for instability for $r \to 0$ is $\Delta \simeq 0{\cdot}91/F$ (Newell 1972) which is below the value of $1/F$ obtained for $r \to 0$. We are interested in the stability of baroclinic flows induced by potential vorticity sources in the presence of small friction but in the absence of baroclinic eddies and we restrict the shear to the range

$$0 \leqslant \Delta \lesssim 0{\cdot}91. \tag{99}$$

For this range of Δ, friction plays a stabilizing role and instability is excluded unless we require that $r = O(\epsilon^{\frac{3}{2}})$. From these considerations it follows that

$$\left.\begin{aligned} \lambda &= \Omega_r(k,l,r)+i\Omega_i(k,l,r),\\ \Omega_r &= k - k\frac{k^2+l^2+F}{(k^2+l^2+2F)(k^2+l^2)} \pm \frac{[\Delta^2(k^2+l^2)^2((k^2+l^2)^2-4F^2)k^2+4F^2k^2]^{\frac{1}{2}}}{2(k^2+l^2)(k^2+l^2+2F)}+O(r^2),\\ \Omega_i &= O(r).\end{aligned}\right\} \tag{100}$$

It has been shown in §2 that a dominant contribution to the solution comes from that part of the spectrum which is most stationary. Consequently we seek to determine the meridional wavenumber l and the corresponding zonal wavenumber k which yield the most stationary phase. The two branches of the dispersion relation (100) are quite complicated, nevertheless they do resemble a cubic with one or three real roots for k if $d\Omega_r(k=0)/dk > 0$ or $d\Omega_r(k=0)/dk \leqslant 0$ respectively. Both branches of (100) are antisymmetric functions of k with $\Omega_r(k=0) = 0$, $d^2\Omega_r(k=0)/dk^2 = 0$; hence the

most stationary phase occurs only for $k = 0$ provided $d\Omega_r(k = 0)/dk = 0$ which from (100) implies that

$$1 - \frac{l^2+1}{(l^2+2)\,l^2} \pm \frac{[\Delta^2 l^4(l^4-4)+4]^{\frac{1}{2}}}{2l^2(l^2+2)} = 0. \tag{101}$$

F has been set equal to 1 since both atmospheric and oceanic flows are characterized by $(U/\beta')^{\frac{1}{2}} \simeq L_R$.

If we set $\Delta = 0$ in (101) we find that $l^2 = 1$ is the only possible solution and it corresponds to the negative branch of (100) or (101). This is the same result as obtained in §2 and we identify this branch as the barotropic mode; the other branch will be referred to as the baroclinic mode. We see that, for $\Delta = 0$ and $l^2 = 1, d\Omega_r(k = 0)/dk = \frac{2}{3}$ for the baroclinic mode which consequently cannot have a phase which is stationary. If we assume that the radicand of (101) does not vanish we obtain that the meridional wavenumber is given by

$$l^2 = [-\tfrac{1}{4}\Delta^2 + [(\Delta^2/4)^2 + 1 - \Delta^2/4]^{\frac{1}{2}}]/(1 - \Delta^2/4), \tag{102}$$

and it corresponds to the barotropic mode of (101). Our relevant range of Δ is defined by (99). For $\Delta = 0{\cdot}91$ (recall that $F = 1$) $l^2 \simeq 0{\cdot}8919$. It follows that the effect of the shear is to slightly decrease the meridional wavenumber of the most stationary phase from the value of $l^2 = 1$ obtained for the pure barotropic case. The baroclinic mode of (100) has positive slope at $k = 0$ for l^2 defined by (102). If the radicand of (101) vanishes then both barotropic and baroclinic modes have zero slope at $k = 0$. We then obtain two conditions which determine both l^2 and Δ

$$l^4 + l^2 - 1 = 0, \quad \Delta^2 = 4l^{-4}(4 - l^4)^{-1}. \tag{103}$$

We find that $l^2 \simeq 0{\cdot}6180$ and $\Delta \simeq 1{\cdot}7013$. This value of Δ is above the threshold of instability for baroclinic eddies and is excluded from our consideration. We conclude that for the range of Δ defined by (99) only the baroclinically modified barotropic mode of the dispersion relation (100) can have a most stationary phase for $k = 0$.

The above considerations indicate that the nature of the instability should be broadly similar to the barotropic case treated earlier. We expect it to be associated with a waveband of $O(\epsilon^{\frac{1}{2}})$ in the vicinity of $k = 0$ and to have a growth rate which is $O(\epsilon^{\frac{3}{2}})$. Consequently we assume that

$$\begin{aligned}
\hat{U}_m &= \hat{U}_m(K, t, t_1, t_2, t_3) = U^0_m + \epsilon^{\frac{1}{2}} U^{\frac{1}{2}}_m + \epsilon U'_m + \epsilon^{\frac{3}{2}} U^{\frac{3}{2}}_m + \dots, \\
\hat{U}_\tau &= \hat{U}_\tau(K, t, t_1, t_2, t_3) = U^0_\tau + \epsilon^{\frac{1}{2}} U^{\frac{1}{2}}_\tau + \epsilon U'_\tau + \epsilon^{\frac{3}{2}} U^{\frac{3}{2}}_\tau + \dots, \\
\hat{V}_m &= \hat{V}_\tau(K, t, t_1, t_2, t_3) = V^0_m + \epsilon^{\frac{1}{2}} V^{\frac{1}{2}}_m + \epsilon V'_m + \epsilon^{\frac{3}{2}} V^{\frac{3}{2}}_m + \dots, \\
\hat{V}_\tau &= \hat{V}_\tau(K, t, t_1, t_2, t_3) = V^0_\tau + \epsilon^{\frac{1}{2}} V^{\frac{1}{2}}_\tau + \epsilon V'_\tau + \epsilon^{\frac{3}{2}} V^{\frac{3}{2}}_\tau + \dots,
\end{aligned} \tag{104}$$

with

$$K = k/\epsilon^{\frac{1}{2}}, \quad t_1 = \epsilon^{\frac{1}{2}} t, \quad t_2 = \epsilon t, \quad t_3 = \epsilon^{\frac{3}{2}} t. \tag{105}$$

The slow times t_1 and t_2 are necessary for a self-consistent approximation. The expressions (104) are substituted into (92)–(95) where terms up to $O(\epsilon^{\frac{3}{2}})$ are retained. This leads to a sequence of problems governing the various orders of ϵ which are solved by suppressing secular terms at each order. We also require the solution to be stationary whenever possible and this leads to selecting the meridional wavenumber according to the rule (102).

The solution at the first three orders leads to the result that

$$\left.\begin{aligned} U_m^0 &= A(K,t_3)+a(K,t_3)e^{-i\lambda t_1}, \quad U_\tau^0 = \gamma A(K,t_3)+\delta a(K,t_3)e^{-i\lambda t_1}, \\ V_m^0 &= B(K,t_3)+b(K,t_3)e^{i\lambda t_1}, \quad V_\tau^0 = \gamma B(K,t_3)+\delta b(K,t_3)e^{-i\lambda t_1}, \end{aligned}\right\} \tag{106}$$

with

$$\lambda = 2K\left(1-\frac{l^2+1}{l^2(l^2+2)}\right), \quad \gamma = \frac{2(1-l^2)}{l^2\Delta}, \quad \delta = \frac{2}{\Delta}\left(\frac{l^2+1}{l^2+2}\right) \tag{107}$$

and l^2 given by (102). We also find that no corrections to the leading order are generated at the second and third orders.

The evolution equations for A, B, a and b are determined by suppressing secular terms at $O(\epsilon^{\frac{3}{2}})$ where the interaction of the leading order of the perturbation field with the field induced by the potential vorticity source finally enters. These evolution equations contain terms which depend on the time scale t_1 through the exponentials $e^{\pm i\lambda t_1}$ (see (106)). (These oscillatory terms are derived from the baroclinic branch of the dispersion relation.) The separation of scales of t_1 and t_3 and the fact that these exponentials have no stationary phase enables us to average these equations over an intermediate time scale θ such that $t_1 \ll \theta \ll t_3$. This leads to the following equations:

$$(\gamma-\delta)\frac{\partial a}{\partial t_3}+iK^3\left(\frac{\gamma}{l^4}-\frac{\delta}{(l^2+2)^2}\right)a+\frac{r}{\epsilon^{\frac{3}{2}}}\left(\gamma-\delta\frac{l^2}{(l^2+2)}\right)a-i\frac{2\Delta K^3}{(l^2+2)^2}a=0, \tag{108}$$

$$(\gamma-\delta)\frac{\partial b}{\partial t_3}+iK^3\left(\frac{\gamma}{l^4}-\frac{\delta}{(l^2+2)^2}\right)b+\frac{r}{\epsilon^{\frac{3}{2}}}\left(\gamma-\delta\frac{l^2}{(l^2+2)}\right)b-i\frac{2\Delta K^3}{(l^2+2)^2}b=0, \tag{109}$$

$$\frac{\partial A}{\partial T}+\left(\frac{R}{\epsilon^{\frac{3}{2}}}+iK^3\right)A=\frac{\hat{G}(0)}{(2\pi)^{\frac{1}{2}}}\int_{-\infty}^{\infty}dK'\,B(K',T), \tag{110}$$

$$\frac{\partial B}{\partial T}+\left(\frac{R}{\epsilon^{\frac{3}{2}}}+iK^3\right)B=-\frac{\hat{G}(0)}{(2\pi)^{\frac{1}{2}}}\int_{-\infty}^{\infty}dK'\,A(K',T), \tag{111}$$

where

$$T = t_3\left[\frac{\delta}{l^4}-\frac{\gamma}{(l^2+2)^2}-\frac{2\Delta}{(l^2+2)^2}\right]\Big/(\delta-\gamma),$$

$$R = (\delta-\gamma l^2/(l^2+2))\left[\frac{\delta}{l^4}-\frac{\gamma}{(l^2+2)^2}-\frac{2\Delta}{(l^2+2)^2}\right]^{-1} \tag{112}$$

$$\hat{G}(0) = l\frac{[\delta-\gamma+\Delta\delta\gamma-\Delta(l^2-2)/(l^2+2)]\,\hat{S}_m(0)-(\delta\gamma-(l^2-2)/(l^2+2))\,\hat{S}_\tau(0)}{\left(\frac{\delta}{l^4}-\frac{\gamma}{(l^2+2)^2}-\frac{2\Delta}{(l^2+2)^2}\right)}.$$

The immediate consequence that emerges from equations (108)–(111) is that for a time scale $t_3 = O(1)$ the dynamics of the barotropic and baroclinic modes is decoupled. Furthermore, the potential vorticity sources do not affect the dynamics of the baroclinic modes which are spun down on this time scale. Hence, it suffices to concentrate on the dynamics of the barotropic mode and to determine the evolution of A and B.

Equations (110) and (111) are identical to equations (37) and (38) with the consequence that the condition for instability, (56), is directly applicable to our present investigation. It follows that instability is triggered if

$$\epsilon > 1{\cdot}5079R^{\frac{2}{3}}/|\hat{G}(0)|, \tag{113}$$

where R and $\hat{G}(0)$ are given in (112).

It is evident from (113) that provided $\hat{G}(0) \neq 0$ the flow field is always unstable in the limit of $r \to 0$. The same conclusion was reached in § 2. If we regard R as a modified friction coefficient then the effect of the shear is to slightly decrease R from 1 for $\Delta = 0$ to 0·8700 for $\Delta = 0{\cdot}91$. The effect on the condition for instability (113) is even smaller. The transformation from t_3 to T is also little affected by the shear. $T/t_3 = 1$ for $\Delta = 0$ and $T/t_3 = 1{\cdot}3303$ for $\Delta = 0{\cdot}91$.

The main difference between the condition for instability of the two-layer model considered here and that derived for the barotropic model lies in the expression for $\hat{G}(0)$ given in (112). The expression for $\hat{G}(0)$ identifies two modes of instabilities; a mode associated with $\hat{S}_m(0)$ and a mode associated with $\hat{S}_\tau(0)$. Each of these modes can separately lead to instability. Nevertheless, the first mode is more efficient than the second mode especially for weak shear. The coefficient of $\hat{S}_m(0)$ in the expression for $\hat{G}(0)$ varies between 1 and 1·1326 when Δ varies between 0 and 0·91. For the same range of Δ the coefficient of $\hat{S}_\tau(0)$ is negative and it varies in magnitude between 0 and 0·4645. These numerical values imply that instabiiity is more easily triggered by the $\hat{S}_m(0)$ mode than by the $\hat{S}_\tau(0)$ mode and that for small values of shear it is unlikely that the flow field can be destabilized by potential vorticity sources which are purely baroclinic.

The combined $\hat{S}_m(0)$–$\hat{S}_\tau(0)$ mode, where both $\hat{S}_m(0)$ and $\hat{S}_\tau(0)$ are present, leads to some interesting results since its effect can be either stabilizing or destabilizing. In the range of Δ considered the coefficient of $\hat{S}_m(0)$ is positive while that of $\hat{S}_\tau(0)$ is negative. It follows that the situation where $\hat{S}_m(0)$ and $\hat{S}_\tau(0)$ have opposite signs is destabilizing since the value of $|\hat{G}(0)|$ increases. This corresponds to the case of a potential vorticity source distribution which decreases in magnitude with height irrespective of whether its barotropic component is cyclonic or anticyclonic (see equation (83)).

When $\hat{S}_m(0)$ and $\hat{S}_\tau(0)$ have the same sign, corresponding to a potential vorticity distribution which increases in magnitude with height, $|\hat{G}(0)|$ decreases yielding a situation which is more stable than the one considered above. In fact, the flow field is stable if $\hat{G}(0) = 0$, which determines a functional relationship between the ratio $\hat{S}_\tau(0)/\hat{S}_m(0)$ and Δ. $\hat{S}_\tau(0)/\hat{S}_m(0)$ decreases monotonically from very large values for $\Delta \to 0$ to the value of 2·4383 for $\Delta = 0{\cdot}91$. It should be emphasized that this neutral curve is not conventional since any deviation from it leads to instability.

The three categories of instabilities discussed above depend on the potential source distribution but their existence is derived from the *barotropic mode* of the dispersion relation, i.e. from the negative branch of (100). The baroclinic modification of the instabilities enters through Δ and it is not directly related to the nature of the potential vorticity sources. The presence of shear introduces coupling between the two modes of (100) which also manifests itself in the zeroth-order field given by (106). The coupling enters through γ and δ both of which are functions of Δ only (see equations (107) and (102)). We observe that the effect of the shear is twofold. It generates γA and γB baroclinic contributions which appear in the expressions for U_τ^0 and V_τ^0. These contributions owe their existence to the barotropic mode. In the range of Δ $(0, 0{\cdot}91)$ γ varies between 0 and 0·2665. The other effect of the shear is to generate barotropic contributions which are proportional to $ae^{-i\lambda t_1}$ and $be^{+i\lambda t_1}$ in the expressions for U_m^0 and V_m^0 in (106). These contributions which are stable (see discussion following (112)) owe their existence to the baroclinic mode. In order to see this we observe that $\delta \to \infty$ when $\Delta \to 0$ ($\delta = 1{\cdot}4378$ for $\Delta = 0{\cdot}91$) which implies that for small shear a and b

should be rescaled to $O(\Delta)$. It follows that in the limit of zero shear the barotropic contribution of the baroclinic mode disappears and the instability field is purely barotropic and is identical to the field analysed in §2. We conclude this section by commenting that the complete spatial structure and temporal evolution of the instability that follow from (110) and (111) can be found in §2.

I should like to thank Prof. V. T. Buchwald for drawing my attention to the important paper by J. J. Mahony, and I am grateful to Dr A. E. Gill and Dr P. B. Rhines for their constructive comments. The inclusion of the numerical examples was suggested by Dr Gill. I should like to thank Mr Z. Greenblatt for making the numerical runs. I am also grateful to Dr N. Liron for helpful discussions. The research was supported by the United States–Israel Binational Science Foundation (BSF), Jerusalem, and by NSF under grant NGR 22-009-727.

REFERENCES

Barnard, B. J. S. & Pritchard, W. G. 1972 Cross-waves. Part 2. Experiments. *J. Fluid Mech.* **55**, 245–255.

Charney, J. G. & Devore, J. G. 1979 Multiple flow equilibria in the atmosphere and blocking. *J. Atmos. Sci.* **36**, 1205–1216.

Coaker, S. A. 1977 The stability of a Rossby wave. *Geophys. Astrophys. Fluid Dyn.* **9**, 1–17.

Erdélyi, A., Magnus, W., Oberhettinger, F. & Tricomi, F. G. 1954 *Tables of Integral Transforms.* McGraw-Hill.

Fjörtoft, R. 1953 On the changes in the spectral distribution of kinetic energy for a two-dimensional, non divergent flow. *Tellus* **5**, 225–237.

Gill, A. E. 1974*a* The stability of planetary waves on an infinite beta-plane. *Geophys. Fluid Dyn.* **6**, 29–47.

Gill, A. E. 1974*b* A fine-scale model of ocean circulation. (Unpublished.)

Gradshteyn, I. S. & Ryzhik, I. M. 1965 *Tables of Integrals, Series and Products.* Academic.

Hogg, N. G. 1973 On the stratified Taylor column. *J. Fluid Mech.* **58**, 517–537.

Huppert, H. E. 1975 Some remarks on the initiation of inertial Taylor columns. *J. Fluid Mech.* **67**, 397–412.

Lorenz, E. N. 1972 Barotropic instability of Rossby wave motion. *J. Atmos. Sci.* **29**, 258–264.

Mahony, J. J. 1972 Cross-waves. Part 1. Theory. *J. Fluid Mech.* **55**, 229–244.

McCartney, M. S. 1975 Inertial Taylor columns on a beta plane. *J. Fluid Mech.* **68**, 71–95.

Merkine, L. 1975 Steady finite-amplitude baroclinic flow over long topography in a rotating stratified atmosphere. *J. Atmos. Sci.* **32**, 1881–1893.

Merkine, L. 1980 Linear and nonlinear resonance of Rossby waves. *Geophys. Astrophys. Fluid Dyn.* **15**, 53–64.

Newell, A. C. 1972 The post bifurcation stage of baroclinic instability. *J. Atmos. Sci.* **29**, 64–76.

Pedlosky, J. 1970 Finite amplitude baroclinic waves. *J. Atmos. Sci.* **37**, 15–31.